Publication status: Preprint has been published in a journal as an article
DOI of the published article: https://doi.org/10.1111/mms.70053

The Vertebral morphology in dolphins (Delphinidae): A 3D approach

María Constanza Marchesi

https://doi.org/10.1590/SciELOPreprints.9197

Submitted on: 2024-06-22
Posted on: 2024-06-27 (version 1)
(YYYY-MM-DD)

Vertebral morphology in dolphins (Delphinidae): A 3D approach

María Constanza Marchesi

Laboratorio de Mamíferos Marinos, Centro Para el Estudio de los Sistemas Marinos (CESIMAR-CONICET), Blvd. Brown 2915, U9120ACD, Puerto Madryn, Chubut, Argentina.

Email: marchesimc@gmail.com

ORCID ID: https://orcid.org/0000-0002-9926-6719

Conflict of interest statement: The author declares that there is no conflict of interest.

ABSTRACT

For almost 90 years, the cetacean vertebral column has puzzled scientists. This is the first 3D geometric morphometric study on the vertebral column of such a numerous group of small odontocetes (24 species). It uses a functional subdivision of the cetacean vertebral column and three landmark configurations to describe and compare vertebral morphology in Delphinidae, relating particular morphologies with the biomechanical requirements of each species. To this end, I assess the effect of size, and that of size and subfamily on vertebral morphology. I also analyzed the statistical differences in shape between species. Phylomorphospaces were created to assess similarities or differences in shape between closely related species with similar/dissimilar habitats. The allometric effect was low in all regions, and there were subfamily-specific allometric effects. Differences between species were greater in the mid-column but this was only partially confirmed statistically, presumably due to low n for some species. The percentage of variance explained by the first two PCs was higher than 58% in all regions, with the torso and the tail stock showing the greatest percentages of

explained variance. The results suggest that the common ancestor of dolphins would have be a non-fast-swimming oceanic species. Coastal habitats seem to have evolved secondarily by means of a reduction in vertebral count, and vertebral morphology associated with greater flexibility (i. e., longer centra, smaller faces). On the contrary, an increased total count and disk-shaped vertebrae were observed to varying degrees in non-coastal species, with the most extreme modifications being found in species with particular habitat specializations. My results support the hypothesis that diversification in vertebral morphology in association to particular habitats was a key factor in delphinid explosive radiation, and provides descriptive basis for analysis of the phylogenetic constrains in vertebral morphology needed to elucidate dolphin diversification and the factors behind it.

KEYWORDS: vertebral shape, vertebral column, dolphin, biomechanics, flexibility, stability.

RESEARCH HIGHLIGHTS

For the first time, this work employs 3D geometric morphometrics to provide a detailed description of vertebral morphology along the vertebral column of 24 dolphin species in order relate particular morphologies with biomechanical requirements of the most specious odontocete family.

INTRODUCTION

Cetaceans are fully aquatic mammals with axial locomotion. Thus, the vertebral column and its associated muscles and tendons play a major role in movement. Given the essential role of the vertebral column in swimming, it has puzzled scientists over the years. The first extensive work on the postcranial anatomy of cetaceans was done by Slijper (1936,) who was the first to allocate cetacean species into locomotor groups ("Stufen") based on vertebral features. This author then went on relating the vertebral structure, as well as muscle development and orientation, with swimming mode (Slijper, 1946; 1961). Afterwards, Crovetto (1991) applied some of Slijper concepts into the study of the vertebral column of large cetaceans. He was the first to use traditional morphometric measurements on cetacean vertebrae. A few years later, Long et al. (1997) studied the vertebral mechanical properties of *Delphinus delphis*, and proposed vertebral designs for stiff and flexible regions of the vertebral column. In addition to this, Pabst's extensive work on dolphin axial muscles facilitated inferences about muscle architecture and function in cetaceans (Pabst, 1990; 1993; 1996; 2000).

It was Emily Buchholtz (1998; 2001) who first integrated all this previous knowledge and analyze the implications of vertebral morphology for locomotor evolution in cetaceans. This author conducted comprehensive reviews of the regional variation of morphology along the cetacean vertebral column from a functional point of view, and proposed functional regions corresponding to morphological changes within the cetacean skeleton. Moreover, three basic morphological patterns of the vertebral column were identified based on centrum shape. These works evidenced the wide spectrum of morphological differences, relating them with particular swimming styles (Buchholtz, 1998; 2001). Later, a complete analysis of vertebral osteology in dolphins was done by employing traditional morphometrics (Buchholtz and Schur, 2004). The regional subdivision, that had been proposed for cetaceans in general, was adapted

for dolphins with anticlinal neural spines (neural spines with a shift in orientation along the vertebral column; Buchholtz and Schur, 2004). Ten years later, Viglino et al. (2014) also employed traditional morphometrics on the vertebral column of seven small odontocete species and reported a strong association between vertebral morphology and phylogeny, rejecting the existence of a relation between vertebral morphology and habitat. These results were later challenged primarily based on the low number of species studied, the significant phylogenetic distance between them, the low number of specimens for each species, and the use of the traditional division of the vertebral column (Marchesi et al., 2017). Traditional morphometrics were posteriorly used to study the role of vertebral modifications in the evolution and speciation of cetaceans (Gillet et al., 2019; 2022). Although they yield valuable results, these two works also employed the traditional division of the vertebral column.

Traditionally, the cetacean vertebral column has been divided into regions or series following boundaries set for terrestrial mammals, grouping vertebrae with similar morphology (and thus, similar function) in animals with quadrupedal terrestrial locomotion (Buchholtz, 1998). This way, it has been usually divided into four regions: cervical, thoracic, lumbar, and caudal (Rommel and Reynolds, 2018). The boundaries can be recognized in both fossil and living cetaceans based on attachment sites (for ribs, pelvis or hemal arches), and in living species by tracing nerve courses and muscle innervations (Slijper, 1936; Buchholtz, 1998). Despite this, axial morphology has dramatically changed during the transition from terrestrial to aquatic environments during the time of archaeocete cetaceans, and again during the subsequent odontocete radiation (Buchholtz and Gee, 2017). As a result, the vertebral column of cetaceans differs from that of terrestrial mammals in morphology and number of vertebrae, and thus, in general morphology and regionalization of the column (Buchholtz, 2001; Cozzi et al., 2016). Buchholtz (2001) proposed the functional

subdivision of the vertebral column for cetaceans. In this sense, recent work has evidenced that dividing the vertebral column based on the regions used for terrestrial mammals might conceal morphological variation particular of cetaceans (Marchesi et al., 2017; 2018). Despite this, several works still adhere to the use of traditional regions.

All these previous osteological works allowed to recognize particular vertebral morphologies that reinforce or limit movements between adjacent vertebrae and affect the flexibility of the vertebral column, and thus, its biomechanical properties (Buchholtz and Schur, 2004; Marchesi et al., 2017, 2020a). In this sense, certain features such as low vertebral count and long centra have been associated with coastal habits; predicting that a high vertebral count would be associated with disk-shaped centra and pelagic habits (Buchholtz and Schur, 2004). Slow swimming species would have morphological features suggesting a more flexible vertebral column whilst pelagic fast swimming species would have osteological features that suggest a more stable column (Woodward, 2006). Regarding vertebral count, the biomechanical significance of a higher number of vertebrae in a region depends on the morphology of the vertebra. In regions with disk-shaped vertebrae, a high vertebral count can enhance stability and store elastic energy (see Pabst, 1996). On the contrary, in regions with spool-shaped vertebrae, a higher number of intervertebral joints can result in more possible bending sites, thus increasing flexibility (Buchholtz and Schur, 2004).

As stated above, the work done on the vertebral column of cetaceans has largely involved traditional morphometrics (Slijper, 1936; Buchholtz, 2001; Buchholtz & Schur, 2004; Viglino *et al.,* 2014; Marchesi et al., 2017; Gillet et al. 2019, 2022). In contrast with traditional morphometrics, geometric morphometrics allows to visualize differences in the shape of complex structures (Zelditch *et al.*, 2004). These methods are better able to capture subtle sources of variation that are not easily summarized

by simple measurements (O'Higgins, 2000; Rohlf, 2000). In particular, three dimensional geometric morphometrics have been widely employed on studies of the cetacean skull (*e.g.*, Galatius et al., 2011; Del Castillo et al., 2014; 2016; 2017; Galatius and Goodall, 2016; Galatius et al., 2020; Coombs et al., 2022) but little has been done on the vertebral column (Marchesi et al., 2020a, 2020b, 2021, 2022).

Delphinidae is the most diverse family of cetaceans and has representatives with quite distinct habitats, from rivers to the open ocean, with species varying locomotor requirements and feeding behaviors. Currently, it includes 38 species (Committee on Taxonomy, 2023), divided into several subfamilies (i.e. Delphininae, Globicephalinae, and Lissodelphininae; McGowen et al., 2020). The high diversity of the family is most likely due to increased rates of diversification during the past 10 Ma (Steeman et al., 2009; do Amaral et al., 2018). It has been suggested that its explosive radiation was due to a combination of vicariant events and adaptation to productive areas caused by the restructuring of oceans during the middle–late Miocene through the Pleistocene (Steeman et al., 2009; Banguera-Hinestroza et al., 2014; do Amaral et al., 2018). Moreover, it is believed that ecological shifts between onshore and offshore habitats, involving changes in vertebral morphology, played a key role for delphinid diversification (Gillet et al., 2022).

In this work, I employed 3D geometric morphometrics to describe vertebral morphology along the vertebral column of 24 delphinid species, analyzing possible morphological similarities or differences between species of the three delphinid subfamilies (Delphininae, Globicephalinae, Lissodelphininae) and two basal delphinids (*Lagenorhynchus acutus* and *L. albirostris*), and relating particular morphologies with the biomechanical requirements of each habitat. This is the first work to describe vertebral morphology in such a numerous group of delphinids with a high level of detail, and focusing on the morpho-functional aspect.

MATERIALS AND METHODS

The specimens included here are part of various mammalogy collections listed in Data S1. I selected only physically adult specimens based on the degree of epiphyseal fusion in the vertebrae (Perrin, 1975; Goodall et al., 1988; Lockyer, Goodall and Galeazzi, 1988). Functional regions were qualitatively determined by the author based on the work of Buchholtz and Schur (2004) and Marchesi et al. (2021). Afterwards, a maximum of five vertebrae were chosen along the vertebral column of each specimen to characterized regions or limits between regions (Figure 1, Table 1). This study included a total of 524 vertebrae from 24 dolphin species (Table 1). In the case of *Tursiops truncatus*, I included only specimens assigned to the coastal "form" (Costa et al., 2022; Data S1).

Due to structural differences in vertebral morphology between regions, three different landmarks configurations containing 28, 35, and 41 landmarks (see Data S2) were obtained with a digitizing arm following a previously published protocol (see Marchesi et al., 2021, 2022). Considering that some regions differ in the number of landmarks, and that I was interested in highlighting differences in the biomechanical aspects, the analyses were performed separately for each vertebral region.

All analyses were done in the free software R v4.1.2 (R Core Team, 2021), using the package Geomorph v4.0.2 (Adams et al., 2021; Baken et al., 2021). An example of the R script used for the study can be found in Data S3. Landmark configurations were superimposed by a Generalized least-squares Procrustes Analysis (GPA; Mitteroecker and Gunz, 2009; Zelditch et al., 2012) using the function *gpagen*, and accounting for the presence of semi-landmarks (see Data S2 and Data S3). During this procedure centroid size (CS) is estimated as a proxy for size.

The function *procD.lm* (Collyer and Adams, 2018, 2021; Adams et al., 2021; Baken et al., 2021) which involves a randomized residual permutation procedure employing the RRPP package v1.3.1 (Collyer and Adams, 2018), was used in two different analysis. First, to evaluate the existence of allometry (shape variation related to size variation) we run two different Procrustes ANOVAS: one using the logarithm of CS (logCS) as the only variable, and one involving the additive linear model of log(CS) and Subfamily (Delphininae, Globicephalinae, Lissodelphininae, and the clade formed by *Lagenorhynchus acutus* - *L. albirostris*). Second, I assessed shape differences between species by running a Procrustes ANOVA on the Procrustes coordinates. After this, pairwise comparisons were done using the function *pairwise* which also involves the above mentioned randomized residual permutation procedure. To evaluate whether differences between species remained after accounting for the common allometric component, a Procrustes ANOVA on the residuals of the additive linear model was also run.

To describe vertebral shape in detail for each species, the mean Procrustes coordinates of shape for each species were plotted using the function *gm.prcomp* to obtain a phylomorphospace (see Collyer and Adams, 2021) in order to qualitatively assess similarities or differences in shape between closely related species with similar/dissimilar habitats. The composed phylogeny employed was based on the work of McGowen (2011) and McGowen et al. (2020), and is depicted in Figure 2.

For inferences about biomechanical requirements and habitats, I classified species into eight different categories (i.e. riverine, coastal-riverine, coastal, oceanic deep-diver, oceanic, fast-swimming oceanic, shelf, and shelf-oceanic species), based on existing literature and previous works (see Figure 2; Jefferson et al. 2015; Würsig et al., 2018; Galatius et al., 2020). For the first three categories, species classification was straightforward. There was only one riverine species in the sample, *S. fluviatilis*,

and one Coastal-riverine species, *S. plumbea*. All *Cephalorhynchus* spp. and *Tursiops truncatus* were considered "coastal". I considered *Globicephala macrorhynchus* the only "oceanic deep-diver" in the sample, given the species preference for feeding at greater depths than any of the other studied species. Species inhabiting oceanic waters and having less than 70 vertebrae were considered as "oceanic", while those having over 70 vertebrae were included within the "oceanic fast-swimming" group. Species that show a strong preference for shelf waters but can get close to the coast were considered as "shelf" species. Finally, the two species in the basal clade, *Lagenorhynchus acutus* and *L. albirostris*, are usually seen forming mixed groups and show a preference for shelf and oceanic waters (ranging from 100 to 1000 meters deep) but can be found close to shore in certain upwelling areas. Based on this, they were considered as a separated group, "shelf-oceanic", despite being fast-swimmer and having over 70 vertebrae.

RESULTS

The allometry analyses showed a low allometric effect in all regions, with size having low but statistically significant z-values. The additive linear model involving size and subfamily also yielded statistically significant values for all regions (Table 2). The results for the Procrustes ANOVA on the Procrustes Coordinates (Table 3) showed statistically significant differences between species for all regions, with the greatest *z*-values being found for the limit between the thorax and the torso, and for the torso. The lowest z-values were observed for the thorax and the tailstock, whilst the synclinal point showed intermediate values. The results on the pairwise comparisons for all species are included in (Data S4). As an overall generalization, species in different quadrants of the morphospace resulted to have statistically significant differences., although caution is recommended when making assertions based on these values

given the low sample size for some species. The results for the Procrustes ANOVA done on the residuals of the additive model also showed great differentiation between species, although with lower z-values in most cases.

The distribution of the species along the first two principal components (PCs) revealed shape similarities between species with similar biomechanical requirements (Figure 3, Data S5). At the same time, it evidenced certain degree of shape similarities between species of very dissimilar habitats. Changes along the first two PCs varied with the region but were mainly related with the length of the centrum, the size of its faces, and the development and orientation of processes and metapophyses (Figure 3). In all cases, the first two PCs explained over 58% of the total variance in vertebral morphology. The mid-torso and the tail stock showed the greatest percentages of explained variance, with 73.5% and 73.7%, respectively. The estimated common ancestor shape (ECAS) for the family is plotted, with most species showing divergence from this estimated shape depending on the region.

At the beginning of the thorax (Th), the ECAS was located close to the origin of coordinates, being most similar to fast-swimming oceanic and shelf/oceanic species (*Lagenorhynchus. albirostris*, *Stenella clymene*, *S. coeruleoalba*). Grouping for Lissodelphininae and Delphininae species seemed to reflect the subfamily grouping, with most species within each subfamily being found in neighboring areas of the morphospace, although some showed particular morphologies (Figure 3). Globicephalinae species were scattered in different areas of the morphospace, these differences were partially observed statistically (Data S4). The two most basal species, *L. albirostris* and *L. acutus*, resulted to be separated in the morphospace, with *L. acutus* diverging greatly from the ECAS (Figure 3). Maximum PC1 values represented long centra with slightly smaller faces, long robust neural processes, and short robust transverse processes with a less anterior inclination (Figure 4, Data S6). This area was

occupied by three groups of species that clearly differed from their closest relatives: the coastal/riverine, *Sousa plumbea,* and the oceanic, S*teno bredanensis*; the riverine *Sotalia fluviatilis* and the coastal *Tursiops truncatus*; and the oceanic deep diver, *Globicephala macrorhynchus*. These groups differed in both in PC1 and PC2 values with maximum PC2 values signaling long centra with smaller faces, neural processes of average length but wider, and short robust transverse processes with a more anterior inclination (Figure 4, Data S6). On the other hand, minimum PC1 values were associated with short centra with large faces, short neural processes but long transverse processes (Figure 4, Data S6), and were observed for for *Lagenodelphis hosei*, which clearly differed from the rest of the species (Figure 3). The remaining Delphininae species evidenced variation along both PC1 and PC2 with *S. longirostris* showing the smallest PC1 values, and *S. frontalis*, *S. attenuata* and *Delphinus delphis* showing the greatest PC1 values (Figure 3). All Lissodelphininae, except *Lagenorhynchus obscurus*, were loosely grouped in the upper left quadrant. *L. obscurus* showed similar PC2 values than *Cephalorhynchus heavisidii* but slightly positive PC1 values. *Lissodelphis peronii* qualitatively differed from the rest of the subfamily, with the most negative PC1 values and the greatest PC2 values, resulting in the most compressed centra of the subfamily. As mentioned above, Globicephalinae showed a great diversity of shapes with *S. bredanensis* having the longest centra and neural process for the subfamily, followed by *G. macrorhynchus* (Data S7). At the opposite extreme, *Grampus griseus* showed the lowest PC1 values for the subfamily, evidencing large faces and short neural processes (Data S7). The fast-swimming species of the subfamily, *Peponocephala electra*, showed values similar to those of *C. hectori* and *L. australis*. Finally, *F attenuate,* was located closed to fast-swimming Delphininae species

In the limit between thorax and torso (ThTo), the coastal *L. australis* was the closest to the origin of coordinates (Figure 3), and the ECAS was located in proximity of this species as well as of some fast-swimming oceanic species. Maximum PC1 values evidenced compressed centra, small faces, slightly shorter neural spines, and long slender transverse processes (Figure 4, Data S6); and were represented by three different groups of fast-swimming and shelf-oceanic species that clearly differed from the rest of their relatives (Figure 3). Variations in PC2 values resulted in *L. hosei* having a small compressed centra with shorter neural spines (but overall well-developed neural processes based on centrum size) and long slender transverse processes with strong posterior inclination (Figure 3, Data S7), and the three Lissodelphininae species with short centra but long neural processes (Figure 3, Data S7). *L. albirostris* and *L. acutus* were statistically different (Data S4), and their PC values suggested differences in the degree compression (Data S7). In this sense, compressed smaller centra and well-developed slender processes were observed for *L. albirostris,* while *L. acutus* showed short centra, although longer than in *L. albirostris*, together with large faces and long robust processes (Data S7). Minimum PC1 values were found for *G. macrorhynchus* and *S. plumbea*, with different negative PC2 values but showing relatively long centra and short but robust transverse processes. All coastal species (Delphininae and Lissodelphininae) are grouped close to the center of the plot but showing different PC2 values. In this sense, *T. truncatus* showed the greatest PC2 values (Figure 3), suggesting longer centra and more robust processes in *T. truncatus*. Shelf and oceanic fast swimming Delphininae species, were scattered widely across the morphospace (Figure 3). The two extremes were seen in *Delphinus delphis* with the greatest PC1 values and resulting in the most compressed centra for the subfamily (Figure 3, Data S6, Data S7), and *S. attenuata* with the minimum PC1 values and evidencing relatively large elongated centra with long neural processes but short

transverse processes. Globicephalinae species were distributed along PC1 and PC2 values with the deep-diver *G. macrorhynchus* with long centra and large robust processes at one extreme, and *G. griseus* with short centra and long slender processes at the other (Figure 3, Data S7). Most Globicephalinae species differed statistically from all Delphininae species, except for species with negative PC1 values and positive PC2 values (*S. plumbea* and *S. fluviatilis*). Most species in this subfamily were statistically different form each other, except for *P. electra* when compared to *F. attenuata* and *G. macrorhynchus* (Data S4).

At the mid-torso (Tm), the oceanic *F. attenuata* showed the shapes closest to the consensus (Figure 3). In this region, the ECAS resulted most similar to an oceanic species (*Grampus griseus*). Maximum PC1 values were associated with longer and overall larger centra (Figure 4, Data S6) and represented by *G. macrorhynchus*, followed by *S. plumbea*. In addition, these species had negative PC2 values which resulted on the longest centra of the family (Data S6, Data S7). Shapes for *L. acutus* and *L. albirostr*is (PC1>0, PC2>0) clearly differed from the rest of the species in having strongly compressed centra whit large faces and slender neural processes, and posteriorly inclined transverse processes. Despite this, they showed statistical differences only when compared to species in different quadrants of the morphospace (Data S4). Most shelf and oceanic fast swimming species (Delphininae and Lissodelphininae) were clustered along negative PC1 values signaling variable degrees of centrum compression, with some species showing positive PC2 values and some negative PC2 values (Figure 3) but not differing statistically from each other (Data S4). Minimum PC1 values were represented by *D. delphis* and three *Stenella* spp. Two oceanic fast swimming species, one belonging to Globicephalinae and one to Lissodelphininae, differ from this general trend (Figure 3). This way, *P. electra* was located close to the coastal *C. hectori* and to other Globicephalinae species, and *L.*

peronii diverged from all other species (Figure 3), although this was not so clearly evidenced statistically (Data S4). Positive PC2 values for *L. peronii* result in transverse processes with posterior inclination. Coastal species formed a loose group around the origin of coordinates, varying both in PC1 and PC2 values (Figure 3). All Lissodelphininae coastal species were relatively close to the origin of coordinates with positive PC1 values, except for *C. heavisidii* that was close to *T. truncatus* (Figure 3). All Globicephalinae species had positive PC1 values and most had negative PC2 values which translated into relatively long centra. The oceanic *S. bredanensis* resulted similar to the riverine species *S. fluviatilis* as they both had long centra, long robust neural processes and short transverse processes with an almost perpendicular orientation with respect to the antero-posterior axis. Despite this, *S. fluviatilis* had considerably longer centra and smaller faces (Data S7). *G. griseus* clearly differed graphically, although not always statistically, from other Globicephalinae species, being located between two coastal species and the two shelf-oceanic species but differing from both groups (Figure 3, Data S4).

Shapes at the synclinal point (SP) showed groups that roughly coincided with the subfamilies, although there were species clearly differing from their closest relatives. Shape similarities between species from the same habitat categories evidenced certain degree of convergence between distantly related species, especially when considering coastal species (Figure 3). In this region, *C. heavisidii* was the closest to the consensus shape, and the ECA was close to this species and other coastal species. Maximum PC1 values were associated with long centra with small faces, short neural processes (long neural arches but short neural spines), and long robust perpendicular transverse processes (Figure 4, Data S4, Data S6). Certain similarities were found between *G. macrorhynchus* and *S. plumbea*, differing in positive PC2 values (Figure 3). Despite these qualitative differences, they did not differ statistically

from species in the same quadrant (Data S4). They both had long centra with the deep diver, *G. macrorhynchus*, showing longer and overall larger centra with notably shorter neural and transverse processes, and *S. plumbea* having long centra with relatively smaller highly convex faces and relatively larger processes (especially the transverse; Data S7). All Delphininae shelf and fast swimming species were grouped along negative PC1 values, with three *Stenella* spp. forming a group. Even though there were little statistical differences between these species, they differed mostly in the degree of centrum compression, with *S. attenuata* and *S. frontalis* having the longest centra, largest faces and longest neural spines but differing in the development of the transverse processes (Data S7), and *S. coeruleoalba* having longer centra with notably larger faces (Data S7). *D. delphis* resembled *S. coeruleoalba* in PC1 values but it was the only Delphinninae species showing negative PC2 values (Figure 3), translating into large faces and a slightly compressed centra. The coastal *T. truncatus* differed greatly from its closest relatives (*S. frontalis*- *S. attenuate*; Data S4) and resulted similar to *C. heavisidii*, which differed in PC2 values with respect to other coastal Lissodelphininae species (Figure 3). Several Lissodelphininae species were grouped close to *L. acutus* (PC1 $\cong$ 0, PC2 $<$ 0), showing variable degrees of centrum compression (Figure 3, Figure 4, Data S7). The coastal *C. hectori* (PC1 $>$ 0, PC2 $<$ 0) and the oceanic fast swimming *L. peronii* (PC1 $\cong$ 0, PC2 $<<$ 0) differed from this group only graphically (Figure 3, Data S4). Differences between these two species where mainly in the size of the faces and the length of the transverse processes being larger and shorter, respectively, in *L. peronii* that in *C. hectori*. In this subfamily, coastal species tended to have longer centra or smaller centrum faces than shelf or oceanic fast swimming species (Data S7). *L. albirostris* differed from other delphinids having highly compressed centra with large faces, long neural processes and shorter transverse processes (Data S7). Globicephalinae species did not show a clear grouping, although

G. griseus and *F. attenuate* were grouped together, with both species showing relatively long centra but with differences in the size of the faces which are relative smaller in the latter species (Figure 3, Data S7). *S. bredanensis* showed longer vertebrae and larger centrum faces than the previous group (Figure 3, Data S7). Finally, *P. electra* also differed from other Globicephalinae (Data S4), being located close to Lissodelphininae species (Figure 3). This species had the most compressed centra and the longest transverse processes for the subfamily (Data S7).

As in the previous analyzed region, in the tailstock (TS) grouping appears to depict the subfamilies, but with certain clustering of species of similar habitats regardless of the subfamily and some species clearly diverging within each subfamily (Figure 3). The estimated common ancestral shape for this region indicates relatively shorter centra than the consensus and similarity with a fast-swimming oceanic species (*P. electra*) and a coastal species (*C. heavisidii*). In this region, shapes for *L. hosei* were the closest to the consensus shape although its centra showed some degree of both antero-posterior and lateral compression, as well as elongation in the dorso-ventral aspect (Data S7). Maximum PC1 values were associated with a highly compressed centra with large flat faces and short neural processes (Figure 4, Data S6). *L. albirostris* and *L. acutus* showed maximum PC1 values, but differed in PC2 values. The differences in PC1 and PC2 values signal both greater lateral and antero-posterior compression, as well as a higher neural process, in *L. albirostris* (Figure 3, Data S7). Despite this, these two species did not differ statistically from each other nor from some Lissodelphininae species (Data S4). At the other end of the axis, minimum PC1 values were found for the coastal/riverine species *S. plumbea*, being the most divergent shape within Delphininae with long centra and small highly convex faces (Figure 3, Data S6, Data S7). Apart from this highly diverging species, Delphinidae species were loosely distributed along negative PC1 and PC2 values, except for *S.*

fluviatilis which showed slightly positive PC2 values (Figure 3). Disregarding this, the riverine species did not show statistical differences with respect to other Delphininae species. The longest centra, smallest faces and a slight dorsoventral compression of the centra were observed for the coastal *Tursiops*. At the other extreme, *L. hosei* had shortest centra with the largest and most convex faces, as well as a clear elongation in the dorsoventral aspect (Data S7). All Lissodelphininae species were grouped together in the upper right quadrant but without showing a clear clustering of habitats within the subfamily, although shelf and oceanic fast swimming species were located in neighboring areas of the morphospace (Figure 3). In this group, only *L. obscurus* statistically differed from the rest of the subfamily (Data S4). Two coastal *Cephalorhynchus* spp. (*C. commersonii* and *C. hectori*) showed the greatest PC1 values within the subfamily, resulting in the most compressed centra and the largest faces for the subfamily (Figure 3, Data S7). The coastal *C. heavisidii* differed greatly from the other *Cephalorhynchus* species, showing lower values both on PC1 and PC2 and resulting in less compressed centra (both antero-posteriorly and laterally) and highly convex faces (Figure 3, Data S7). Finally, Globicephalinae species were widely distributed in the morphospace with *G. macrochynchus* and *G. griseus* located in neighboring areas and showing distinct shape with respect to the other species (Figure 3). Both these species had long but overall small centra with highly convex faces, especially *G. macrorhynchus* (Data S7). *F. attenuate* and *S. bredanensis*, grouped together close to the riverine *S. fluviatilis*. They all had long centra but differed in the size of the faces, with the riverine species having the longest vertebrae, the largest faces and an almost circular cross section (centrum width similar to centrum height; Data S7). The oceanic fast swimming *P. electra*, differed greatly from other Globicephalinae species, both graphically and statistically (Data S4), being located close to the oceanic fast swimming Lissodelphininae species but also to the coastal *C.*

heavisidii (Figure 3). Once more, this species was the one that showed the most compressed centra (both antero-posteriorly and laterally) within the subfamily (Data S7).

DISCUSSION

Almost a hundred years have passed since Slijper (1936) first works on cetacean anatomy. He stated the basis from which numerous researchers have expanded the knowledge regarding the vertebral column of this particular group of mammals with axial locomotion (e.g., Buchholtz, 2001; Buchholtz and Schur, 2004, Marchesi et al. 2020b, and references therein). It has been shown that the radical reorganization of the cetacean vertebral column has resulted in a non-coincidence of traditional series boundaries and functional units of the column (Buchholtz and Schur, 2004). In this sense, the cetacean column may be subdivided based on its own structural discontinuities. Buchholtz and Schur (1998, 2001) proposed the recognition of the functional vertebral series for cetaceans which subdivides the “traditional” lumbar and caudal regions into a torso, a tail stock and a fluke. This functional subdivision evidences differences in morphology along the vertebral column of dolphins that could be obscured when considering the traditional subdivision (Marchesi et al., 2017; 2018). In this work, I provide a vertebral formula for this functional subdivision for 24 dolphin species (DataS1) as well as detailed results of 3D geometric morphometric analyses of particular vertebra, signaling these functional regions, along the skeleton to evidence a great diversity in vertebral morphology both along the vertebral column and between species within the most numerous odontocete family. I adhere to the suggestion made by Buchholtz and Schur (2004) that future eco-morphological analyses of cetacean vertebral column should consider the particular diversity of shapes along the cetacean vertebral column. Despite this, I acknowledge the difficulty

of assessing functional regions in different species and recognize the need to collect or gather morphometric data throughout the entire column for correct assessment.

Recently, it has been proposed that the most recent common ancestor (MRCA) of crown delphinids and that of each delphinid subfamily (Lissodelphininae, Globicephalinae, and Delphininae) lived in offshore environments (Gillet et al., 2022). In this work, for all the analyzed regions, the positionof the estimated ancestor in the morphospace, and its resulting shape, suggested that the MRCA of crown delphinids was most likely an oceanic non-fast-swimming odontocete.

Across the family, the degree of morphological variations arising from the ancestral oceanic shape showed extremes. On the one hand, species with high stability requirements (e.g. long-distance fast-swimming species; *L. hosei, L. acutus, L. albirostris*, *Lissodelphis* sp.), evidenced a tendency to centrum shortening, increased relative size of the vertebral faces as well as of the processes. On the other hand, species with high flexibility requirements (*G. macrorhynchus*, *S. fluviatilis*, *S. plumbea*) showed a lengthening of the vertebral centra, reduction of the size of the faces and low short, or well-developed, processes depending on the species particular habitats. In this sense, requirements for flexibility are usually associated with highly heterogenous environments such as shores and rivers, but they may arise also in the oceanic depths with heterogenous distribution of highly mobile prey, as was evidenced by the vertebral morphology of *G. macrorhynchus*. In the Canary Islands, Soto et al. (2008) found that short-finned pilot whales feed on mesopelagic highly evasive prey (predominantly squid) through short fast deep dives (15 min, 800 m) that involve a relatively fast descent (2 m/s), several fast sprints and an ascent (2.2 m/s). In this species, the large size and vertebral morphology (long centra with robust but relatively shorter processes in proportion to the centra) might be related with this diving pattern that involves fluke movements both during ascent and descent and fast vertical

sprinting. Apart from these morphological extremes, this study evidenced a wide array of morphologies in association to habitats and biomechanical requirements. In each functional region, particular morphologies would suggest that delphinid speciation was mediated by changes in vertebral morphology with species with similar habitat requirements showing some degree of morphological convergence also evidenced by Gillet et al. (2022).

Buchholtz and Schur (2004) proposed that oceanic dolphin species would have higher total counts of compressed vertebrae and that this would be the derived state in delphinids, while coastal habitats would be associated with lower total counts of elongated centra and would represent the ancestral state. My results partially supported this hypothesis since the two earliest diverging delphinid species, *L. acutus* and *L. albirostris*, showed the most compressed centra and the longest neural processes in most of the regions, as well as two of the greatest total vertebral counts, with *L. acutus* having over 80 vertebrae and *L. albirostris*, having over 90 vertebrae (Data S1). Vertebral shape in these species differed notably from the estimated ancestor for the family, suggesting that speciation involved notable changes in vertebral morphology. In this sense, some convergence in vertebral shape has been reported for *L. albirostris* and the fast-swimming oceanic porpoise *Phocoenoides Dalli*, in which total count reaches up to 97 vertebrae, the maximum for any odontocete (Marchesi et al., 2022). On the other hand, coastal species showed lower total count and longer vertebra, and they qualitatively differed from their closest oceanic estimated ancestor in most regions, although there was variation depending on the region and the species. Differences in total count and vertebral morphology have been also evidenced for the coastal *T. truncatus* suggesting, in agreement with genetic studies, that coastal *Tursiops* populations emerged from offshore individuals that specialized in exploiting resources in shallower waters (Natoli et al., 2004; Moura et al., 2013;

Costa et al., 2020). Thus, in accordance to Gillet et al. (2022), the present study suggests that adaptation to the coastal environment would have happened secondarily and independently within Delphininae and Lissodelphininae during the Pliocene (Banguera-Hinestroza et al., 2014), and having a coastal habitat would not be an ancestral character in this group of highly diverse odontocetes. In this sense, coastal habitats and their associated morphological traits in porpoises also showed to be secondarily derived traits associated with the evolution of sister clades in both hemispheres (Marchesi et al. 2022). Similar processes could be behind this adaptation in Delphinidae and Phocoenidae (Galatius et al., 2010). It has been proposed that the small size associated with coastal habitats could be mediated by paedomorphosis, as has been evidenced for *C. commersonii* and *Phocoena phocoena* (Galatius et al., 2010). In these species, morphological changes may be mediated by species-specific allometry (Galatius et al., 2010), which plays an important role in vertebral morphology (Marchesi et al. 2021). In relation to this, the results in this paper suggest that size has little relevance in the overall shape variation within Delphininae. Despite this, we found subfamily-specific allometry, thus, the effect of size on vertebral shape varies from one subfamily to the other and it may represent relevant component of shape variation in some regions. Different levels of allometry need to be investigated for these species to assess the effect of size in vertebral morphology and how changes in shape mediated by changes in size may have been involved in delphinid speciation.

Delphinids are included in the third pattern of vertebral variation described by Buchholtz (2001) for cetaceans, having extremely compressed vertebrae along most of the torso in addition to tail stock with relatively long centra. This general morphological pattern would translate into a stable torso from which the flexible peduncle oscillates. This restricted flexibility is especially notable in the two most basal species which show morphological features associated with high stability in the

tailstock, suggesting that flexibility would be mostly restricted to the junction between tailstock and fluke (ball vertebrae; Fish et al., 2006). Although most delphinids follow this basic pattern of a stable torso and a flexible tailstock, vertebral morphology across Delphinidae showed to be highly variable. Factors underlying these variations remain to be studied. In some regions, vertebral morphology seemed to be relatively influenced by phylogeny with species from the same subfamily in neighboring areas of the morphospace, especially at the extremes of the vertebral column (e.g. anterior thorax, synclinal point and tail stock). Despite this, some species showed particular morphologies associated to certain habitats that would be related with species diversification (Gillet et al., 2022). What is more, areas considered the most relevant in generating propulsive forces and increasing efficiency of swimming muscles, namely the limit between thorax and torso and the mid torso (ThTo, Tm; see Buchholtz, 2001; Buchholtz and Schur, 2004; Marchesi et al., 2020), were the ones showing the greatest morphological differences of the five analyzed regions. In this regions, closely related species with different habitats clearly differed from each other. Despite this, it should be acknowledged that, given the differential involvement of each functional region in the different types of swimming (see Buchholtz and Schur, 2004; Marchesi et al., 2020), similar requirements may be resolved by the several different combinations of vertebral variation along the vertebral column.

It has been argued that the thorax is a highly conserved region along the postcranial skeleton of dolphins and whales (Piscitelli et al., 2010; Marchesi et al., 2021). In this work, the anterior thorax seemed to be the most preserved region, with most species being close to the consensus shape and to the estimated ancestor shape. Despite this, morphological differences were found for species with habitats that differ from that of their proposed ancestor. The deep-diving *G. macrorhynchus*, the riverine species *S. fluviatilis*, and the coastal-riverine *S. plumbea*; showed relatively

longer vertebrae in all regions and varied in the development of processes overall resulting in a relatively more flexible union between the cervical region and the thorax. This could increase maneuverability at the expense of energy expenditure of maintaining the head stable when swimming, but it would be highly valuable when feeding in heterogenous environments (Fish et al. 2003). On the other hand, two fast-swimming species (oceanic and shelf-oceanic) showed extremely compressed vertebrae as it would be expected based on the requirement to stabilize the head during long distance oceanic fast swimming. In this sense, it has been widely shown that there is an evolutive tendency for a shortening of cervical vertebra in fully aquatic mammals (Buchholtz 2001). Even though I am not including cervical vertebrae in the present study due to difficulties to obtain comparable landmark configurations, in these species, the extremely shortened first thoracic vertebrae could particularly enhance cervical rigidity; and thus, aid in stabilizing the neck during prolonged fast-swimming as well as when catching schooling fish in open waters.

In most dolphin species, the torso functions as a unit in the generation of forces that move the tail (Buchholtz and Schur 2004, Marchesi et al. 2017, 2020). It includes vertebrae that are classically defined as posterior thoracic, as well as, lumbar sacral and caudal vertebrae (Buchholtz and Schur 2004). In this work, I have included three different sections of the torso which allowed me to make an exhaustive analysis of vertebral morphology along this biomechanically highly relevant region. In particular, both the beginning (ThTo) and the middle of the torso (Tm) are especially important regions since it is there where the large forces that are transmitted to the posterior region of the column are developed by the longissimus muscle (Pabst 1993). Buchholtz and Schur (2004) introduced the term “lumbarization” to refer to the changes suffered by vertebrae adjacent to the lumbar region through which they attain features that are typical of lumbar vertebrae (i.e., disk-shaped and long processes). The results of the

present work showed that these typically lumbar features are more extremely marked in species with high stability requirements such as shelf-oceanic, shelf, and oceanic fast-swimming species which show a disk-shape morphology and long slender processes extended throughout the whole torso.

In the torso, the orientations and lengths of neural arches and spines are proposed to be correlated with the anatomy and importance of longissimus and multifidus musculature (Slijper 1936; Marchesi et al. 2020). In this sense, when compared to coastal species, species with requirements for speed and prolonged swimming (shelf, shelf-oceanic and oceanic) showed longer processes, especially the neural ones, which would provide a longer lever arm and mechanical advantage for the longissimus muscle fibers. In addition to this, the inclination of transverse processes also showed patterns associated with a greater stability in fast-swimming species (shelf and oceanic), in which processes had a strong anterior inclination in the mid torso. Not only does this stiffen the vertebral column but it also increases the lever arm for the muscles attached to those structures (see Marchesi et al. 2020). It is worth mentioning that three fast-swimming species, namely *L. acutus*, *L. albirostris* and *L. peronii*, showed posteriorly inclined transverse processes which suggest that different strategies to stiffen the torso appeared independently during dolphin diversification. In this sense, it has been shown that swimming style diversity allows the possibility that particular vertebral patterns and their functional results may have evolved multiple times through dolphin evolution (Buchholtz 2001). Conversely, in species with requirements for high flexibility (coastal, riverine, oceanic, deep-divers), the almost perpendicular orientation of the transverse processes throughout the torso would potentially create areas with greater rotational potential as has been previously proposed for the coastal *L. australis* (Marchesi et al. 2017).

In delphinids, the synclinal point is the transition between the stable torso and the flexible tailstock and it represents the area where muscle forces affecting the fluke's angle of attack are produced (Slijper, 1936; Buchholtz and Schur, 2004; Pabst, 1990; Marchesi et al., 2017). In this sense, species with high flexibility requirements (riverine, coastal/estuarine, and coastal) resulted to have longer processes, especially the transverse ones. This could be reflecting a greater development of the muscles involved in the rotational and lateral movements of the tail, giving to these species certain advantage for the rotation of the fluke, a requirement for inhabiting and catching prey in highly heterogenous habitats (Marchesi et al. 2017). In this region, the apparent correspondence between subfamilies and the areas of the morphospace, with some species converging with species of different subfamilies but similar habitats, suggests that the basic shape for this region might be constrained by phylogeny, although some degree of plasticity allowed changes in vertebral shape in accordance to habitat requirements.

Finally, the tails stock, is considered to be the most flexible region along the vertebral column of delphinids (Buchholtz, 2001, Marchesi et al. 2017). In this area, vertebral morphology seemed to be highly restricted by phylogeny, given that most species for each subfamily were located in similar areas of the morphospace. Despite this, species with similar flexibility requirements shared morphological features such as long centra with convex faces and well-developed neural processes (e.g., *G. griseus*; *G. macrorhynchus*, and *S. plumbea*). As mentioned above, the two basal species (*L. acutus* and *L. albirostris*) had extremely disk-shaped vertebrae with flat large faces, extending the "lumbarization" to the tailstock probably as an extreme adaptation to fast-swimming. Two *Cephalorhynchus* species also showed disk-shaped vertebrae with large faces, but in this case the convexity of the faces would suggest increased flexibility in the tailstock of these coastal species.

Even though this work is mostly descriptive, the detailed analysis of vertebral morphology in such a numerous group of dolphin species with various habitats has allowed me to characterize vertebral shape and infer differences related with different habitat requirements. Despite this, there is a great deal of variation between species grouped into a particular habitat. These differences could be reflecting fin-scale partitioning between sympatric species, since they may be related with prey size and/or differences in spatial distribution and habitat use (Bearzi, 2005; Gillet et al. 2022; Spitz et al. 2006; Smith et al. 2008). The apparent lack of differences between species with dissimilar habitats could also be due to the subjectivity involved in asserting only one type of habitat for these wide-ranging species. It is worth mentioning that care should be applied when making inferences using discrete categories for a continuous and complex factor such as habitat/habits. Further investigations relating continuous ecological parameters are needed to clarify the effect of habitat requirements on vertebral morphology.

CONCLUSION

This is the first work to study vertebra morphology in such a numerous group of dolphin species. In agreement with previous work, it suggest that the common ancestor of dolphins would have been a non-fast-swimming oceanic species and that further morphological variation would be associated with the particular habitat of the species. In this sense, coastal habitats seem to have evolved secondarily from oceanic ancestors by means of a reduction in vertebral count, and vertebral morphology suggesting greater flexibility. On the contrary, an increased total count and disk-shaped vertebrae were observed to varying degrees in non-coastal species, with the most extreme modifications being found in fast-swimming which differed greatly from the estimated ancestral oceanic habitat. This work adds support to the previously

proposed hypothesis stating that diversification in vertebral morphology and total count was a key factor in delphinid explosive radiation involving independent secondary adaptation of some species to coastal environments and a specialization for pelagic fast swimming in others. Despite this, further studies involving dated phylogenies and a deeper analysis of the phylogenetic constrains is necessary to elucidate dolphin diversification and the factors behind it.

ACKNOWLEDGMENTS

I want to particularly acknowledge Dr. Rolando González-José, who provided the Microscribe, and Dr. Mariano Coscarella, for being my advisors during my doctoral and postdoctoral fellowships. Data collection for this work was possible thanks to funding from the Society for Marine Mammalogy (Small Grants in Aid of Research, 2018). I want to express my appreciation to collection curators and museum staff for assistance during specimen preparation and data collection. I especially thank to Dr. Darrin Lundee and John Ososky at the US National History Museum, Smithsonian Institution; to Marisa Surovy at the AMNH; to Sergio Lucero and Dr. Pablo Teta at MACN; and to Nestor García from CENPAT; Argentina. Finally, I would like to dedicate this paper to the memory of Dr. Natalie R. Prosser Goodall: a great leader and mentor, without whom this would not have been possible.

AUTHOR CONTRIBUTIONS

María Constanza Marchesi: Conceptualization; data curation; formal analysis; funding acquisition; investigation; methodology; project administration; resources; visualization; writing – review and editing.

FUNDING

CONICET, Argentina: Postdoctoral Fellowship

Society for Marine Mammalogy: Small Grants in Aid of Research

Science and Technology Ministry (MINCyT), Argentina: PICT 2019 - 2160

DATA AVAILABILITY

The datasets presented in this study can be found in online repositories, https://doi.org/10.6084/m9.figshare.25246378

REFERENCES

Adams, D. C., Collyer, M. L., Kaliontzopoulou, A., and Baken, E.K. (2021). Geomorph: Software for geometric morphometric analyses. R package version 4.0.2. https://cran.r-project.org/package=geomorph.

Baken, E. K., Collyer, M. L., Kaliontzopoulou, A., and Adams, D. C. (2021). Geomorph v4.0 and gmShiny: enhanced analytics and a new graphical interface for a comprehensive morphometric experience. Methods in Ecology and Evolution. Methods in Ecology and Evolution, 12: 2355–2363. https://doi.org/10.1111/2041-210X.13723

Banguera-Hinestroza, E., Hayano, A., Crespo, E. A., and Hoelzel, A. R. (2014). Delphinid systematics and biogeography with a focus on the current genus Lagenorhynchus: multiple pathways for antitropical and trans-oceanic radiation. Molecular Phylogenetics and Evolution, 80: 217–230. https://doi.org/10.1016/j.ympev.2014.08.005

Bearzi, M. (2005). Dolphin sympatric ecology. Marine Biology Research, 1: 165–175.https:// doi.org/10.1080/17451000510019132

Buchholtz, E. A. (1998). Implications of vertebral morphology for locomotor evolution in early Cetacea. In J. G. M. Thewissen (Ed.), The emergence of whales:

Evolutionary patterns in the origin of Cetacea (pp. 325–351). Plenum Press. https://doi.org/10.1007/978-1-4899-0159-0_11

Buchholtz, E. A. (2001). Vertebral osteology and swimming style in living and fossil whales (order: Cetacea). Journal of Zoology, 253: 175–190. https://doi.org/10.1017/s0952836901000164

Buchholtz, E. A., and Schur, S. A. (2004). Vertebral osteology in Delphinidae (Cetacea). Zoological Journal of the Linnean Society, 140: 383–401. https://doi.org/10.1111/j.1096-3642.2003.00105.x

Buchholtz, E. A. (2007). Modular evolution of the cetacean vertebral column. Evolution and Development, 9: 278–289. https://doi.org/10.1111/j.1525-142X.2007.00160.x

Buchholtz, E. A., and Gee, J. K. (2017). Finding sacral: Developmental evolution of the axial skeleton of odontocetes (Cetacea). Evolution and Development, 19: 190–204. https://doi.org/10.1111/ede.12227

Collyer, M. L., and Adams, D. C. (2018). RRPP: An R package for fitting linear models to high-dimensional data using residual randomization. Methods in Ecology and Evolution, 9(2): 1772–1779. https://besjournals.onlinelibrary.wiley.com/doi/10.1111/2041-210X.13029

Collyer, M. L., and Adams, D. C. (2021). RRPP: Linear Model Evaluation with Randomized Residuals in a Permutation Procedure. https://cran.r-project.org/web/packages/RRPP

Committee on Taxonomy. (2023). List of Marine mammal species and subspecies. Society for Marine Mammmalogy, www.marinemammalscience.org, consulted on October 1st, 2023.

Coombs, E. J., Felice, R. N., Clavel, J., Park, T., Bennion, R. F., Churchill, M., Geisler, J. H. Beatty, B., and Goswami, A. (2022). The tempo of cetacean cranial evolution. Current Biology, https://doi.org/10.1016/j.cub.2022.04.060

Costa, A. P. B., McFee, W., Wilcox, L. A., Archer, F. I., and Rosel, P. E. (2022). The common bottlenose dolphin (*Tursiops truncatus*) ecotypes of the western North Atlantic revisited: an integrative taxonomic investigation supports the presence of distinct species. Zoological Journal of the Linnean Society, 1608–1636. https://doi.org/10.1093/zoolinnean/zlac025

Cozzi, B., Huggenberger, S., and Oelschläger, H. A. (2016). Anatomy of dolphins: insights into body structure and function. Academic Press.

Crovetto, A. (1991). Etude osteometrique et anatomo-funcionelle de la colonne vertebrale chez grans cetaces [Osteometric and anatomofunctional study of the vertebral column in large cetaceans]. Investigations on Cetacea, 23, 71–89.

del Castillo, D. L., D. A. Flores, and Cappozzo, H. L. (2014). Ontogenetic development and sexual dimorphism of Franciscana dolphin skull: a 3D geometric morphometric approach. Journal of Morphology, 275: 366–1375. https://doi.org/10.1002/jmor.20309

del Castillo, D. L., Segura, V., Flores, D.A., and Cappozzo, H. L. (2016). Cranial development and directional asymmetry in Commerson's dolphin, *Cephalorhynchus commersonii commersonii*: 3D geometric morphometric approach. Journal of Mammalogy, 97:1345-1354

del Castillo, D. L., Viglino, M., Flores, D.A., and Cappozzo, H. L. (2017) Skull ontogeny and modularity in two species of *Lagenorhynchus*: morphological and ecological implications. J Morphol 278:203–214

do Amaral, K.B., Amaral, A.R., Ewan Fordyce, R., and Benites Moreno, I. (2018). Historical Biogeography of Delphininae Dolphins and Related Taxa (Artiodactyla: Delphinidae). Journal of Mammalian Evolution, 25: 241–259. https://doi.org/10.1007/s10914-016-9376-3

Fish, F. E., Nusbaum, M. K., Beneski, J. T., and Ketten, D. R. (2006). Passive cambering and flexible propulsors: cetacean flukes. Bioinspiration & Biomimetics, S42. https://doi.org/10.1088/1748-3182/1/4/506

Fish, F. E., Peacock, J., and Rohr, J. (2003). Stabilization mechanism in swimming odontocete cetaceans by phased movements. Marine Mammal Science, 19: 515–528. https://doi.org/10.1111/j.1748-7692.2003.tb01318.x

Galatius, A. (2010). Paedomorphosis in two small species of toothed whales (Odontoceti): How and why? Biological Journal of the Linnean Society, 99: 278–295. https://doi.org/10.1111/j.1095-8312.2009.01357.x

Galatius, A., Berta, A., Frandsen, M. S., and Goodall, R. N. P. (2011). Interspecific variation of ontogeny and skull shape among porpoises (Phocoenidae). Journal of Morphology, 272(2): 136–148. https://doi.org/10.1002/jmor.10900

Galatius, A., Racicot, R., McGowen, M., and Olsen, M. T. (2020). Evolution and diversification of delphinid skull shapes. Iscience, 23(10). https://doi.org/10.1016/j.isci.2020.101543

Galatius, A., and Goodall, R. N. P. (2016). Skull shapes of the Lissodelphininae: radiation, adaptation and asymmetry. Journal of Morphology, 277: 776-785. https://doi.org/10.1002/jmor.20535

Gillet, A., Frédérich, B., and Parmentier, E. (2019). Divergent evolutionary morphology of the axial skeleton as a potential key innovation in modern cetaceans. Proceedings of the Royal Society B, 286: 20191771. https://doi.org/10.1098/rspb.2019.1771

Gillet, A., Frédérich, B., Pierce, S.E., and Parmentier, E. (2022) Iterative habitat transitions are associated with morphological convergence of the backbone in delphinoids. Journal of Mammalian Evolution, 29: 931–946. https://doi.org/10.1007/s10914-022-09615-7

Goodall, R. N. P., Galeazzi, R. A., Leatherwood, S., Miller, K. W., Cameron, I. S., Kastelein, R. K., and Sobral, A. P. (1988). Studies of Commerson's dolphins, *Cephalorhynchus commersonii*, off Tierra del Fuego, 1976–1984, with a review of information of the species in South Atlantic. In R. L. Brownell and G. P. Donovan (Eds.), Reports of the international whaling commission, special issue 9 (pp. 3–70). International Whaling Commission.

Jefferson, T. A., Webber, M. A., and Pitman, R. L. (2015). Marine mammals of the world: A comprehensive guide to their identification. Academic Press.

Lockyer, C., Goodall, R. N. P., and Galeazzi, R. A. (1988). Age and body length characteristics of *Cephalorhynchus commersonii* from incidentally caught specimens off Tierra del Fuego. Report of the International Whaling Commission, 9: 103–118.

Long, J. H., Jr., Pabst, D. A., Shepherd, W. R., and McLellan, W. (1997). Locomotor design of dolphin vertebral columns: Bending mechanics and morphology of *Delphinus delphis*. Journal of Experimental Biology, 200: 65–81. https://doi.org/10.1242/jeb.200.1.65

Marchesi, M. C., Mora, M. S., Pimper, L. E., and Goodall, R. N. P. (2017). Can habitat characteristics shape vertebral morphology in dolphins? An example of two phylogenetically related species from southern South America. Marine Mammal Science, 33: 1126–1148. https://doi.org/10.1111/mms.12432

Marchesi, M. C., Mora, M. S., Crespo, E. A., Boy, C. C., Gonzalez-José, R., and Goodall, R. N. P. (2018). Functional subdivision of the vertebral column in four south american dolphins. Mastozoología Neotropical, 25: 329– 343. http://doi.org/10.31687/saremmn.18.25.2.0.12

Marchesi, M. C., Mora, M. S., Dans, S. L., Coscarella, M. A., and Gonzáles González-José, R. (2020b). Vertebral morphology in partially sympatric dolphins: A 3D

approach. Frontiers in Marine Science, 7: 581762. https://doi.org/10.3389/fmars.202.581762

Marchesi, M. C., Boy, C. C., Dans, S. L., Mora, M. S., and González-José, R. (2020a). Morphology of the vertebral centra in dolphins off the south western South Atlantic: A 3D morphometric approach and functional implications. Marine Mammal Science, 36: 548–564. https://doi.org/ 10.1111/mms.12660

Marchesi, M. C., Dans, S. L., Mora, M. S., and González-José, R. (2021). Allometry and ontogeny in the vertebral column of southern hemisphere dolphins: A 3D approach. Journal of Mammalian Evolution, 28: 125–134. https://doi.org/10.1007/s10914-020-09514-9

Marchesi, M. C., Galatius, A., Zaffino, M., Coscarella, M. A., and González-José, R. (2022). Vertebral morphology in extant porpoises: Radiation and functional implications. Journal of Morphology, 283(3): 273–286. https://doi.org/10.1002/jmor.21441

McGowen, M. R. (2011). Toward the resolution of an explosive radiation—a multilocus phylogeny of oceanic dolphins (Delphinidae). Molecular Phylogenetics and Evolution, 60(3): 345–357.

McGowen, M., Tsagkogeorga, G., Álvarez-Carretero, S., dos Reis, M., Struebig, M., Deaville, R., Jepson, P. D., Jarman, S., Polanowski, A., Morin, P. A., and Rossiter, S. J. (2020). Phylogenomic Resolution of the Cetacean Tree of Life Using Target Sequence Capture. Systematic Biology, 69 (3): 479-50. https://doi.org/10.1093/sysbio/syz068

Mitteroecker, P., and Gunz, P. (2009). Advances in geometric morphometrics. Evolutionary biology, 36: 235–247. https://doi.org/10.1007/s11692-009-9055-x

Moura, A. E., Nielsen, S. C. A., Vilstrup, J. T., Moreno-Mayar, J. V., Gilbert, M. T. P., Gray, H. W. I., Natoli, A., Möller, L., and Hoelzel, A. R. (2013) Recent diversification of a marine genus (*Tursiops* spp.) tracks habitat preference and environmental change. Systematic Biology, 62: 865–877. https:// doi. org/ 10. 5061/ dryad. k501d

Natoli, A., Peddemors, V. M., and Hoelzel, A. R. (2004) Population structure and speciation in the genus *Tursiops* based on microsatellite and mitochondrial DNA analyses. Journal of Evolutionary Biology, 17:363–375. https://doi.org/10.1046/j.1420-9101.2003.00672.x

Pabst, D. A. (1990). Axial muscles and connective tissues of the bottlenose dolphin. In S. Leatherwood and R. R. Reeves (Eds.), The bottlenose dolphin (pp. 51–67). Academic Press. https://doi.org/10.1016/B978-0-12- 440280-5.50007-X

Pabst, D. A. (1993). Intramuscular morphology and tendon geometry of the epaxial swimming muscles of dolphins. Journal of Zoology, 230: 159–176. https://doi.org/10.1111/J.1469-7998.1993.TB02679.X

Pabst, D. A. (1996). Springs in swimming animals. American Zoologist, 36: 723–735. https://doi.org/10.1093/icb/36.6.723

Pabst, D. A. (2000). To bend a dolphin: Convergence of force transmission designs in cetaceans and scombrid fishes. American Zoologist, 40(1): 146–155. http://dx.doi.org/10.1093/icb/40.1.146

Perrin, W. F. (1975). Variation of spotted and spinner porpoises (genus *Stenella*) in the eastern tropical Pacific and Hawaii. Bulletin of the Scripps Institution of Oceanography, 21, 206.

Piscitelli, M. A., McLellan, W. A., Rommel, S. A., Blum, J., Barco, S. G., and Pabst, D. A. (2010). Lung size and thoracic morphology in shallow (*Tursiops truncatus*) and deep (*Kogia* spp.) diving cetaceans. Journal of Morphology, 271: 654–673.

R Core Team (2021). R: A language and environment for statistical computing. R Foundation for Statistical Computing, Vienna, Austria. https://www.R-project.org/.

Rommel, S. A., and Reynolds, J. E. (2018). Skeleton. In B. Würsig, J. G. M. Thewissen, and K. M. Kovacs (Eds.) Encyclopedia of Marine Mammals, 3rd Edition (pp. 861–871). Academic Press.

Slijper, E. J. (1936). Die Cetaceen, Vergleichend-Anatomisch und Systematisch [the cetaceans, compared anatomy and systematics]. Capita Zoologica, 7.

Slijper, E. J. (1961). Locomotion and locomotory organs in whales and dolphins (Cetacea). Symposia of the Zoological Society of London, 5: 77–94.

Slijper, E. J. (1946). Comparative biologic anatomical investigations on the vertebral column and spinal musculature of mammals. Tweede Sectie, 17: 1-128.

Smith, B. D., Ahmed, B., Mowgli, R. M., and Strindberg, S. (2008). Species occurrence and distributional ecology of nearshore cetaceans in the Bay of Bengal, Bangladesh, with abundance estimates for Irrawaddy dolphins *Orcaella brevirostris* and finless porpoises *Neophocaena phocaenoides*. Journal of Cetacean Research and Management, 10: 45–58.

Soto, N. A., Johnson, M. P., Madsen, P. T., Díaz, F., Domínguez, I., Brito, A., and Tyack, P. (2008). Cheetahs of the Deep Sea: Deep Foraging Sprints in Short-Finned Pilot Whales off Tenerife (Canary Islands). Journal of Animal Ecology, 77(5): 936–947. http://www.jstor.org/stable/20143270

Spitz, J., Rousseau, Y., and Ridoux, V. (2006). Diet overlap between harbor porpoise and bottlenose dolphin: an argument in favour of interference competition for food? Estuarine Coastal and Shelf Science, 70: 259–270. https://doi.org/10.1016/j.ecss.2006.04.020

Steeman, M.E., Hebsgaard, M.B., Fordyce, R.E., Ho, S.Y.W., Rabosky, D.L., Nielsen, R., Rahbek, C., Glenner, H., Sørensen, M.V., and Willerslev, E. (2009). Radiation

of extant cetaceans driven by restructuring of the oceans. Systematic Biology, 58: 573–585. https://doi.org/10.1093/sysbio/syp060

Viglino, M., Flores, D. A., Ercoli, M. D., and Álvarez, A. (2014). Patterns of morphological variation of the vertebral column in dolphins. Journal of Zoology, 294: 267–277. https://doi.org/10.1111/jzo.12177

Woodward, B. (2006). Locomotory Strategies, Dive Dynamics, and Functional Morphology of the Mysticetes: Using Morphometrics, Osteology, and DTAG Data to Compare Swim Performance in Four Species of Baleen Whales. (PhD thesis), University of Maine.

Würsig, B., Thewissen, J. G. M., and Kovacs, K. M. (Eds.) (2018). Encyclopedia of Marine Mammals. Academic Press. https://doi.org/10.1016/C2015- 0-00820-6

Zelditch, M. L., Swiderski, D. L., Sheets, H. D., and Fink, L. (2004). Geometric Morphometrics for Biologists: A Primer. San Diego: Elsevier.

Table 1. Sample size for each region of the studied species. The number of the vertebrae (counted from the first cervical vertebra) employed to characterize each particular region for each species is shown between parentheses. See Figure 1 for region names.

	Th	ThTo	Tm	SP	TS
L. acutus	6 (8)	7(21)	8(42)	8(58)	8(66)
L. albirostris	3(8)	3(22)	4(46)	3(65)	3(73)
C. commersonii	14(8)	10(20)	12(36)	12(44)	13(50)
C. heavisidii	1(8)	1(20)	1(36)	1(42)	1(50)
C. hectori	1(8)	1(20)	1(36)	1(41)	1(50)
L. australis	4(8)	2(20)	1(36)	1(45)	-
L. cruciger	5(8)	5(20)	5(36)	4(50)	3(57)
L. peronii	1(8)	1(22)	1(43)	1(56)	1(66)
L. obscururs	8(8)	8(20)	6(36)	5(50)	7(57)
F. attenuata	4(8)	8(18)	6(34)	7(44)	6(54)
G. griseus	4(8)	4(20)	4(36)	4(45)	4(55)
G. macrorhynchus	1(8)	1(18)	1(30)	1(35)	1(43)
P. electra	5(8)	6(20)	6(42)	6(50)	6(65)
S. bredanensis	5(8)	8(19)	8(34)	6(44)	6(53)
L. hosei	1(8)	1(21)	1(41)	1(56)	1(64)
S. attenuata	5(8)	5(20)	5(42)	5(58)	2(64)
S. plumbea	1(8)	1(20)	1(29)	1(34)	1(40)
D. delphis	8(8)	8(21)	8(39)	8(53)	7(60)
S. clymene	5(8)	5(20)	5(38)	5(52)	5(58)
S. coeruleoalba	5(8)	4(20)	5(40)	6(56)	6(62)
S. fluviatilis	2(8)	2(20)	2(30)	2(39)	2(43)
S. frontalis	7(8)	6(20)	7(36)	8(50)	8(56)
S. longirostris	7(8)	7(20)	7(38)	8(51)	8(60)
T. truncatus	5(8)	5(19)	5(32)	5(40)	5(47)
Total	108	109	110	109	105

Table 2. Results for the Procrustes ANOVA of the linear models including: 1) size (log (CS)), and 2) size (log (CS)) and subfamily (SF). Degrees of freedom (DF), percentage of explained variance (%), and Z values for each studied region: thorax (Th), limit thorax-torso (ThTo), mid-torso (Tm), synclinal point (SP), and tail stock (TS). Statistical significance is demarked by asterisks next to Z values; * $p < 0.05$; ** $p \leq 0.01$; *** $p \leq 0.001$.

	1) PC vs log(CS)			2) PC vs log(CS)+SF		
	DF	%	Z	DF	%	Z
Th						
log(CS)	1	4.14	3.24**	1	2.64	2.59**
SF				3	19.13	6.04**
R	106	95.86		103	76.73	
ThTo						
log(CS)	1	6.44	3.798**	1	9.27	5.556**
SF				3	22.33	6.945**
R	107			104	71.23	
Tm						
log(CS)	1	7.11	3.11**	1	2.46	2.908**
SF				3	40.67	6.618**
R	108	92.89		105	52.22	
SP						
log(CS)	1	8.65	4.38**	1	3.53	4.199**
SF				3	34.90	11.268**
R	107	91.35		108	56.45	
TS						
log(CS)	1	7.07	2.84**	1	4.76	4.02**
SF		92.93		3	43.14	6.25**
R	103			100	49.80	

Table 3. Results for the Procrustes ANOVA of shape versus species (Sp) done on the 1) Procrustes coordinates, and on the 2) residuals of the additive linear model involving size and subfamily. Degrees of freedom (DF), R squared (R^2), F and Z values for each studied region: thorax (Th), limit thorax-torso (ThTo), mid-torso (Tm), synclinal point (SP), and tail stock (TS). Statistical significance is marked by asterisks; * $p < 0.05$; ** $p \leq 0.01$.

		1			2		
	DF	%	F	Z	%	F	Z
Th							
Sp	23	56.12	4.67	9.82**	44.05	2.87	8.316**
R	84	43.88			55.95		
ThTa							
Sp	23	70.99	9.05	17.28**	59.44	5.42	11.835**
R	85	29.01			40.56		
Tm							
Sp	23	83.99	19.61	15.51**	69.09	8.36	7.29**
R	86	16.01			30.91		
SP							
Sp	23	77.03	12.39	12.91**	59.59	5.45	14.56**
R	85	22.96			40.41		
TS							
Sp	22	74.72	11.02	10.67**	48.99	3.58	10.38**
R	82	25.28			51.01		

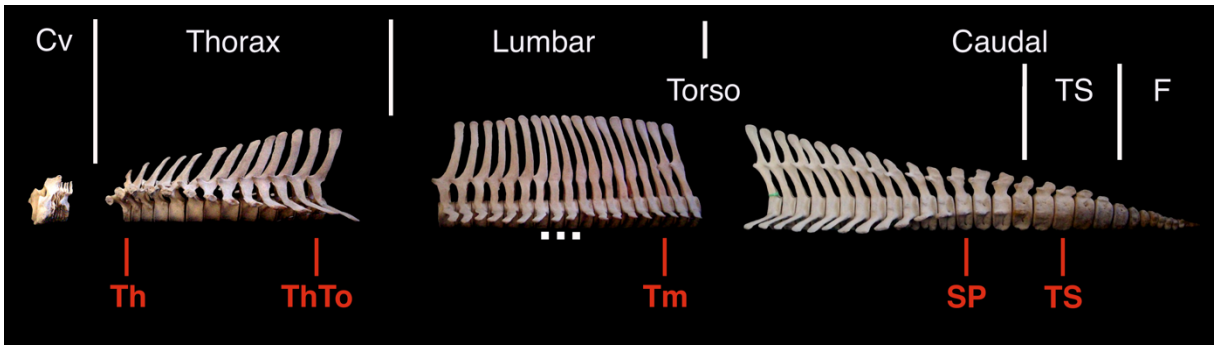

Figure 1. Skeleton of the hourglass dolphin (*Lagenorhynchus cruciger*) depicting both traditional and functional regions and the position of the five different vertebrae selected for the study. Cv: cervical region; Th: anterior thorax; ThTo: limit between thorax and torso, Tm: mid-torso; SP: synclinal point; TS: tailstock; F: fluke. Scale = 5 cm.

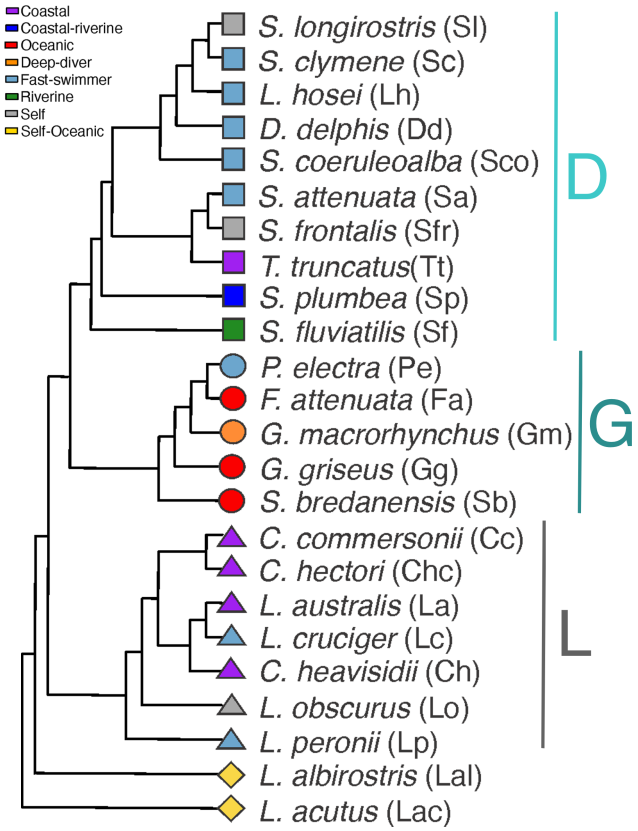

Figure 2. Composed phylogeny used in the study. Based on McGowen (2011) and McGowen et al. (2020). It includes different colors and symbols according to habitat and subfamily, respectively. Vertical bars denote subfamilies. It also contains abbreviations used for species in subsequent figures and tables. For full names on the species, see Data S1.

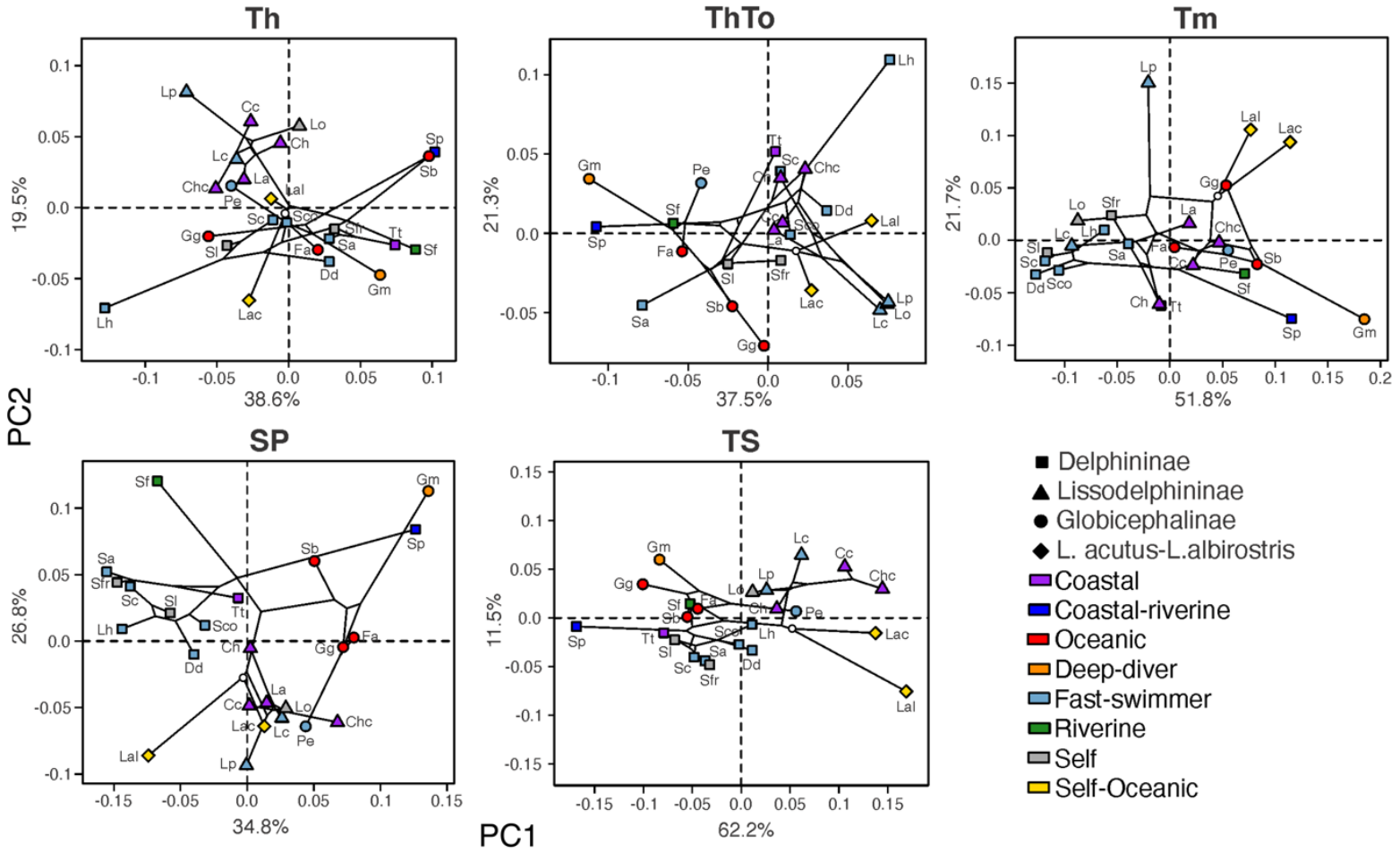

Figure 3. Plot of the first two principal components (PC1 and PC2) resulting from mapping the phylogeny onto species mean shapes (PC-scores), and the reconstructed scores for nodes and root (white circle). The percentage of explained variance is depicted for each PC and region. Tip colors refer to the habitat of each species and tip shapes correspond to the subfamily. The white circles with black edges represent the estimated ancestral shapes for the family. See Figure 1 for region names and Figure 2 for abbreviations of species names.

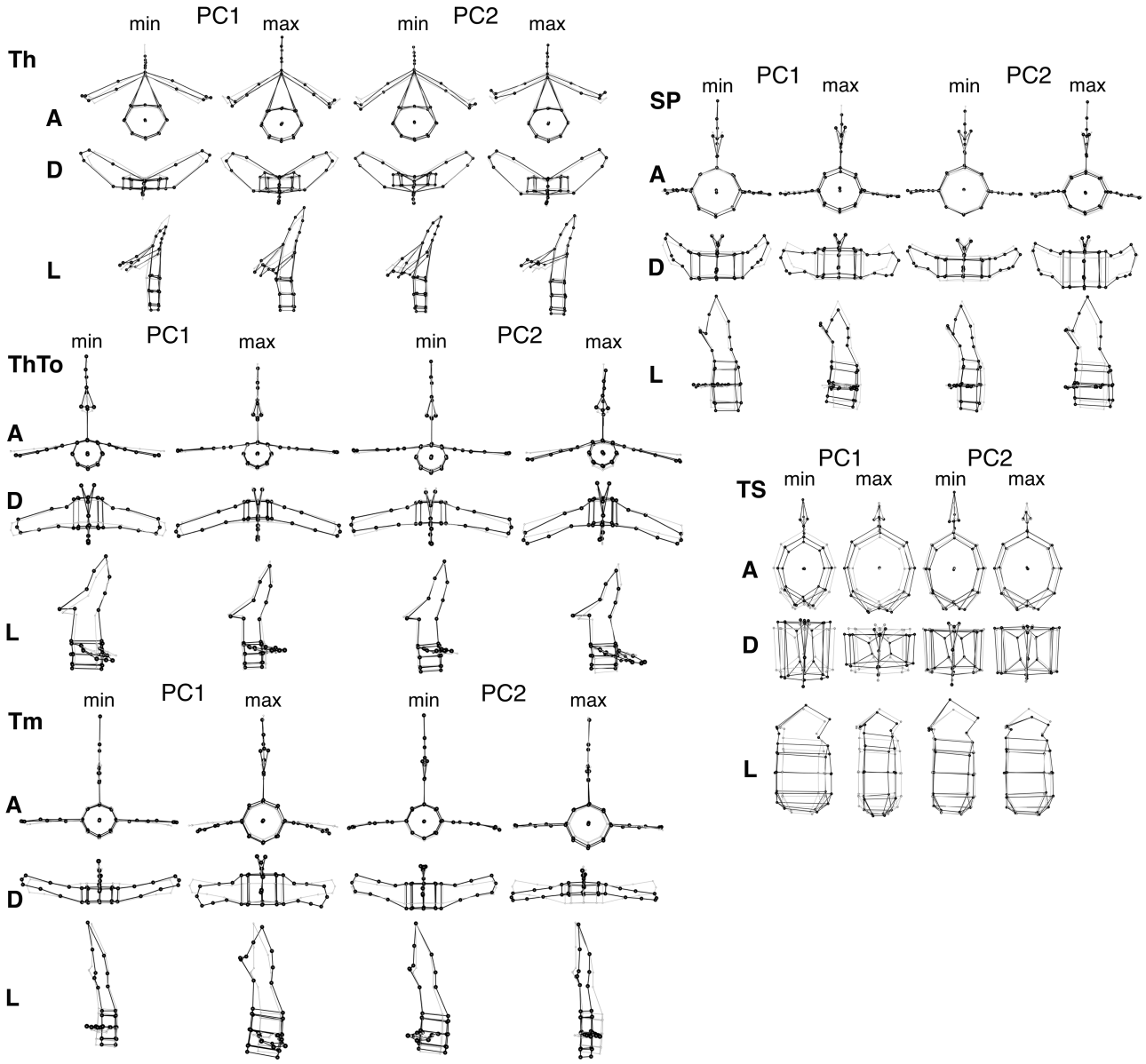

Figure 4. Wireframes of vertebral shapes associated with minimum and maximum values (black markers and lines) of the first two principal components (PC1 and PC2) in comparison to the consensus shape for all species (grey markers and lines). For each region, anterior (A), dorsal (D), and left lateral (L) views are included. See Figure 1 for region names.

Data S1. Collection ID numbers for the specimens included in the study. AMNH: American Museum of Natural History, New York, U.S.A.; CNP-MAM and LAMAMALO: Laboratorio de Mamíferos Marinos of the Centro para el Estudio de los Sistemas Marinos, CESIMA-CONICET, Puerto Madryn; CZIP: Instituto de la Patagonia of the Universidad de Magallanes, Punta Arenas, Chile ; NMNZ: (kept at Acatushún); UFSC: Universidade Federal de Santa Catarina, Brasil; RNP: Museo Acatushún de Aves y Mamíferos Australes, Ushuaia; USNM: United States National Museum of Natural History, Smithsonian Institution, Washington D.C., U.S.A. TR: traditional regions; FR: Functional regions; TC: total vertebral count; TL: total length in cm; T: thoracic; L: lumbar; Cd: caudal; To: torso; TS: tailstock; F: fluke. *Specimens kept at Museo Acatushún.

Museum Code	TR	FR	TC	TL	Sex
Cephalorhynchus commersonii					
RNP 634	C7T13L14Ca30+	Cv7T13To28TS5F11+	64+	145.5	F
RNP 636	C7T13L13Ca31	Cv7T13To27TS5F12	64	136	M
RNP 637	C7T13L14Ca29+	Cv7T13To28TS6F9+	63+	130.2	M
RNP 648	C7T13L14Ca23+	Cv7T13To27TS6F4+	57+	129	M
RNP 651	C7T13L14Ca30	Cv7T13To26TS6F12	64	140+	---
RNP 653	C7T13L14Ca28	Cv7T13To26TS5F11	62	131.4	F
RNP 675	C7T13L14Ca26+	Cv7T13To27TS6F6+	59+	---	F
RNP 1169	C7T13L14Ca31	Cv7T13To27TS6F12	65	122+	M
RNP 1466	C7T13L14Ca28	Cv7T13To26TS5F10+	62	132+	M
RNP 1910	C7T13L15Ca23+	Cv7T13To27TS6F4+	57+	133	M
RNP 2119	C7T12L15Ca25+	Cv7T12To27TS6F5+	57+	123.5	M
RNP 2181	C7T12L14Ca32	Cv7T12To28TS6F12	65	132+	---
RNP 2200	C7T12L14Ca26+	Cv7T12To28TS6F6+	59+	134	M
RNP 2246	C7T13L14Ca30	Cv7T13To27TS5F12	64	132.5	M
RNP 2670	C7T12L14Ca30	Cv7T12To27TS6F11	63	139	F
USNM 550154	C7T13L14Ca29+	Cv7T13To26TS6F11+	63+	132	F
USNM 550156	C7T12L14Ca32	Cv7T12To28TS6F12	65	136	M
Cephalorhynchus heavisidii					
USNM 550067	Cv7T12L15Cd34	Cv7T12To26TS6F13+	68	169	M
Cephalorhynchus hectori					
NMNZ1804*	Cv7T13L14Cd29+	Cv7T13To26TS6F13+	65	---	M
Delphinus delphis					
AMNH 185364	Cv7T14L20Cd22+	Cv7T14To35TS7F11	74	228.6	M
USNM 500263	Cv7T14L21Cd33+(1)	Cv7T14To37TS7F10+(1)	75+(1)	168	F
USNM 500267	Cv7T14L21Cd32+(2)	Cv7T14To38TS7F8+(2)	74+(2)	182	F
USNM 500273	Cv7T14L20Cd31+(2)	Cv7T14To34TS7F10+(2)	72+(2)	179	M
USNM 550201	Cv7T14L19Cd33	Cv7T14To35TS7F10	73	210	M
USNM 550450	Cv7T14L21Cd32+(2)	Cv7T14To36TS7F10+(2)	74+(2	204	F
USNM 550470	Cv7T14L20Cd33	Cv7T14To35TS7F11	74	211	F
USNM 571207	Cv7T14L20Cd34	Cv7T14To35TS7F12	75	210	F
Feresa attenuata					
MACN 20472	Cv7T11L17Cd14+	Cv7T11To31TS+	49+	222.8	F
USNM 504916	Cv7T11L16Cd32+	Cv7T11To31TS8F9+	66+	---	---
USNM 504918	Cv7T11L15Cd35	Cv7T11To32TS7F11	68	203	---
USNM 571268	Cv7T11L16Cd36	Cv7T11To33TS8F11	70	223	M
USNM 593895	Cv7T11L16Cd33+	Cv7T11To33TS7F9+	67+	196.5	F
USNM 594072	Cv7T11L16Cd34+	Cv7T11To33TS7F10+	68+	207	M
USNM 594386	Cv7T11L15Cd23+	Cv7T11To32TS6+	56+	---	M
USNM 594387	Cv7T11L16Cd32+	Cv7T11To32TS7F9+	66+	---	M
Grampus griseus					
USNM 504328	Cv7T13L15Cd34	Cv7T13To32TS6F11+	69	291	M

USNM 550383	Cv7T13L16Cd33	Cv7T13To32TS6F11+	69	298	M
USNM 550393	Cv7T13L15Cd33	Cv7T13To32TS6F10	68	---	M
USNM 550407	Cv7T13L17Cd32+	Cv7T13To33TS6F10+	69+(1)	288	M
Globicephala macrorhynchus					
USNM 504395	Cv7T11L12Cd15+	Cv7T13To25TS5+	45+	381	F
Lagenorhynchus acutus					
USNM 550995	Cv7T14L20Cd38+	Cv7T14To41TS6F11+	79+	253	M
USNM 571326	Cv7T15L19Cd38+	Cv7T15To43TS6F9+	79+	259	M
USNM 571395	Cv7T15L19Cd40	Cv7T15To41TS6F12+(1)	81+	242	M
USNM 571445	Cv7T14L20Cd31+	Cv7T14To41TS6F4+	72+	---	---
USNM 593685	Cv7T15L20Cd40	Cv7T15To42TS612	82	278	M
USNM 593696	Cv7T14L20Cd40	Cv7T15To42TS6F12	81	250	M
USNM 593724	Cv7T14L20Cd35+	Cv7T15To42TS6F7+	76+	255	M
USNM 594139	Cv7T14L20Cd31+	Cv7T14To41TS6F4+	72+	270	M
Lagenorhynchus albirostris					
USNM 550208	Cv7T15L24Cd45	Cv7T15To47TS8F14	91	238	F
USNM 593990	Cv7T15L24Cd45	Cv7T15To47TS8F14	91	242	F
USNM 594163	Cv7T15L22Cd19+	Cv7T15To41+	63+	259	M
USNM 594176	Cv7T14L23Cd39+	Cv7T14To47TS8F7+	83+	255	F
Lagenorhynchus australis					
RNP 0179	C7T13L15Ca29+	Cv7T13To29TS5F8+	62+	---	---
RNP 0719	C7T14L15Ca28+	Cv7T14To30TS6F7+	18+	199	H
RNP 0753	C7T14L15Ca31	Cv7T14To30TS5F11	67	193+	H?
RNP 2128	C1T11+	C1T11+	64+	---	---
Lagenorhynchus cruciger					
CNPMAMM 0641	C7T13L19Ca33	Cv7T13To33TS5F13	71	178	M
CZIP1080	C7T13L19Ca25+	Cv7T13To34TS5F6+	65+	---	---
RNP 2217	C7T13L18Ca33	Cv7T13To34TS5F12	71	172+	M
RNP 2366	C7T13L18Ca32	Cv7T13To33TS5F12	70	178.5	M
RNP 2717	C7T14L19Ca33	Cv7T14To34TS5F12	72	173.5	M
Lagenodelphis hosei					
USNM 571619	Cv7T14L18Cd38+	Cv7T14To40TS5F11+	77+	227	F
Lissodelphis peronii					
RNP 1713	Cv7T15L27Cd33	Cv7T15To41TS7F12	82	---	---
Lagenorhynchus osbcurus					
CNPMAMM100578	Cv7T13L20Cd30+	Cv7T13To34TS6F10+	70+	174	H
CNPMAMM100597	Cv7T13L19Cd33	Cv7T13To34TS6F12	72	159	---
CNPMAMM100780	Cv7T13L17Cd32+	Cv7T13To33TS5F11+	69+	175	M
LAMAMALO 062	Cv7T13L17Cd12+	Cv7T13To29+	49+	---	---
LAMAMALO 079	Cv7T13L18Cd29+	Cv7T13To34TS5F8+	67+	169	M
LAMAMALO 082	Cv7T13L18Cd32+	Cv7T13To34TS5F11+	70+	171	H
LAMAMALO 084	Cv7T13L19Cd32+	Cv7T13To34TS6F11+	71+	---	H
LAMAMALO 088	Cv7T13L18Cd31+	Cv7T13To33TS5F11+	69+	---	H
RNP 1104	Cv7T13L18Cd30+	Cv7T13To33TS6F10+	68+	---	---
Peponocephala electra					
USNM 550399	Cv7T13L16Cd43+	Cv7T13To43TS6F10+	79+	246	F
USNM 593799	Cv7T13L15Cd44+	Cv7T13To43TS6F10+	79+	246	M
USNM 593941	Cv7T13L16Cd38+	Cv7T13To42TS6F6+	74+	246	M
USNM 593999	Cv7T13L16Cd42+	Cv7T13To41TS7F10+	78+	249.5	M
USNM 594059	Cv7T13L16Cd42+	Cv7T13To42TS6F10+	78+	248	M
USNM 594070	Cv7T13L16Cd42+	Cv7T13To43TS6F9+	78+	247.8	M
Stenella attenuata					
USNM 395390	Cv7T14L20Cd40	Cv7T14To41TS6F13	81	218	M
USNM 395391	Cv7T14L20Cd38+	Cv7T14To41TS6F10+	79+	203	M
USNM 396028	Cv7T14L20Cd37	Cv7T14To39TS7F11	78	197	M
USNM 500122	Cv7T14L18Cd40	Cv7T14To40TS6F12	79	195	F
USNM 550016	Cv7T14L19Cd20+	Cv7T14To39+	60+	193	M

Steno bredanensis					
USNM 504462	Cv7T12L13Cd33	Cv7T12To29TS6F11	65	215	F
USNM 504465	Cv7T13L14Cd32+	Cv7T12To29TS6F11+	66+	228	M
USNM 504466	Cv7T12L14Cd31+	Cv7T12To31TS5F9+	66+	218	F
USNM 504467	Cv7T12L15Cd32+	Cv7T12To31TS5F11+	66+	235	M
USNM 504468	Cv7T12L15Cd31+	Cv7T13To30TS5F11+	65+	227	M
USNM 504487	Cv7T13L14Cd29+	Cv7T13To28TS5F10+	63+	221	F
USNM 550221	Cv7T12L14Cd29+	Cv7T12To30TS5F8+	62+	215	F
USNM 550837	Cv7T13L13Cd33+	Cv7T13To29TS6F11+	66+	228	M
Stenella clymene					
USNM 550510	Cv7T13L19Cd33	Cv7T13To35TS6F11	72	174	M
USNM 550532	Cv7T13L18Cd35	Cv7T13To36TS6F11	73	184	M
USNM 550534	Cv7T13L18Cd32+	Cv7T13To35TS6F9+	70+	195	M
USNM 550536	Cv7T13L19Cd34	Cv7T13To37TS6F10	73	186	M
USNM 550540	Cv7T13L19Cd22+	Cv7T13To36TS5+?	61+	186	M
Stenella coeruleoalba					
USNM 571267	Cv7T13L20Cd36+	Cv7T13To39TS6F11+	76+	219	M
USNM 593553	Cv7T13L20Cd34+	Cv7T13To40TS6F8+	74+	225	---
USNM 593612	Cv7T13L18Cd35+	Cv7T13To41TS6F6+	73+	209	F
USNM 593658	Cv7T13L20Cd36+	Cv7T13To41TS6F9+	76+	224	M
USNM 593723	Cv7T14L20Cd36+	Cv7T14To39TS7F10+	77+	217	F
USNM 593763	Cv7T13L20Cd39	Cv7T13To40TS7F12	79	216	F
Sotalia fluviatilis					
UFSC 1074*	Cv7T13L9Cd26	Cv7T13To20TS6F10	56	---	F
USNM 571558	Cv7T13L9Cd23+	Cv7T13To20TS5F7+	52+	187	M
Stenella frontalis					
USNM 500858	Cv7T13L17Cd33	Cv7T13To33TS5F12	70	208	F
USNM 504321	Cv7T13L17Cd27+	Cv7T13To34TS5F5+	64+	192	F
USNM 504736	Cv7T13L18Cd19+	Cv7T13To32TS5	57+	210	F
USNM 504758	Cv7T13L17Cd35	Cv7T13To33TS5F14	72	201	M
USNM 550376	Cv7T13L18Cd30+	Cv7T13To33TS5F10+	68+	216	M
USNM 571512	Cv7T14L17Cd31	Cv7T14To32TS5F11	69	176	M
USNM 571513	Cv7T13L18Cd32	Cv7T13To33TS6F11	70	181	M
AMNH 63779	Cv7T13L16Cd22+	Cv7T13To32TS6	58	---	---
Stenella longirostris					
USNM 395414	Cv7T14L17Cd34+	Cv7T14To36TS6F9+	72+	173	M
USNM 482843	Cv7T13L18Cd34	Cv7T13To35TS6F11	72	173	F
USNM 500017	Cv7T14L16Cd35+	Cv7T14To35TS7F9+	72+	174	F
USNM 500018	Cv7T14L17Cd36	Cv7T14To36TS7F10	74	167	M
USNM 500019	Cv7T13L18Cd33+	Cv7T13To34TS7F9+	71+	180	M
USNM 500020	Cv7T14L18Cd34+	Cv7T14To36TS7F9+	73+	175	M
USNM 504922	Cv7T14L17Cd31+	Cv7T14To34TS6F8+	69+	173	M
USNM 594181	Cv7T14L17Cd33+	Cv7T14To33TS7F10+	71+	178.5	F
Sousa plumbea					
USNM 550941	Cv7T12L9Cd22+	Cv7T12To18TS5F8+	50+	---	M
Tursiops truncatus					
USNM 504121	Cv7T12L14Cd26+	Cv7T12To26TS6F8+	59+	249	F
USNM 504123	Cv7T12L14Cd19+	Cv7T12To27TS5F1+	52+	232	F
USNM 550364	Cv7T12L14Cd27+	Cv7T12To26TS6F9+	60+	258	F
USNM 550440	Cv7T12L13Cd26+	Cv7T12To24TS6F8+	58+	264	F
USNM 571845	Cv7T12L13Cd28	Cv7T12To25TS6F10	60	273	F

Data S2. Wireframe visualization of the landmark configurations employed in the study, following Marchesi et al. (2022). A) Landmarks obtained on Th; B) Landmarks obtained on ThTo, Tm, and SP; C) Landmarks obtained on TS. See Figure 1, for region names. # : order in which landmarks were digitized. In bold, landmarks on the anterior epiphyses; underlined, landmarks on the posterior epiphyses. L: left; NA: neural arch; NS: neural spine; R: right; TP: transverse process; proximal or distal with respect to the centrum. * indicate landmarks taken by projecting radiated figures. In each region, shapes correspond to the mean shape of the sample. Landmarks taken on the posterior (caudal aspect of the vertebra) are shown in red. Dorsal and left lateral views show landmarks on the transverse and neural processes, respectively. The dorsal view in C is not included given the absence of transverse processes.

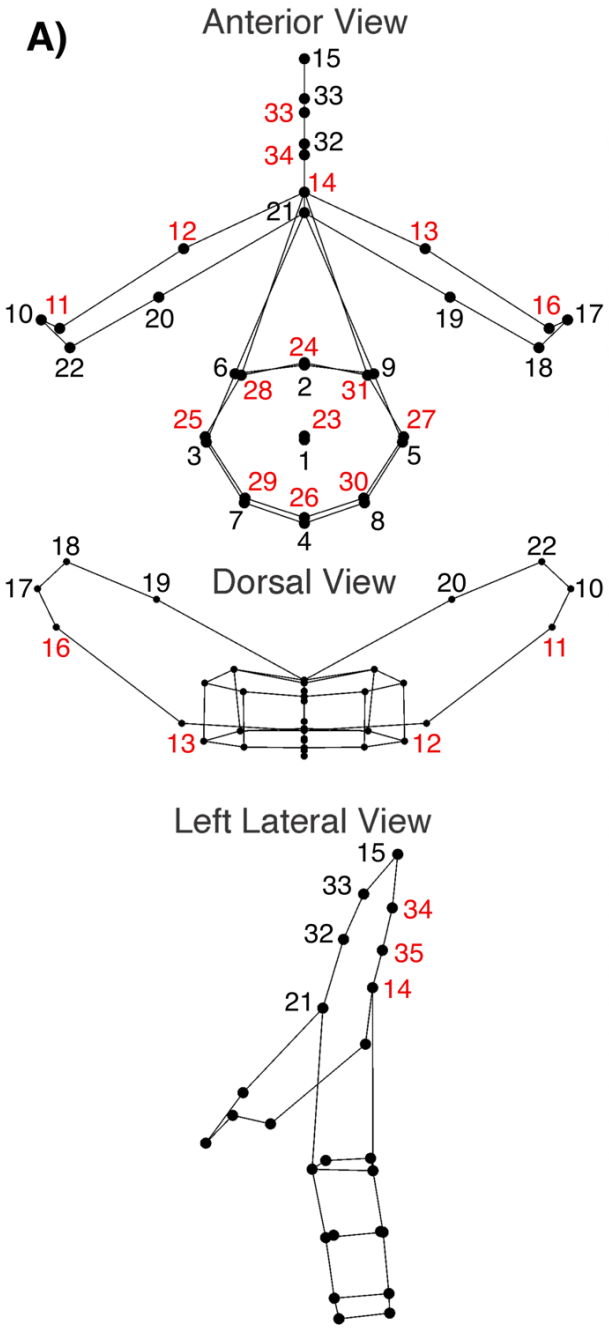

#	Description
1	**Center of anterior epiphysis**
2	**Mid-point on dorsal border of anterior epiphysis***
3	**Mid-point on R lateral border of anterior epiphysis***
4	**Mid-point on ventral border of anterior epiphysis***
5	**Mid-point on L lateral border of anterior epiphysis***
6	**Mid-point between 2 and 3***
7	**Mid-point between 3 and 4***
8	**Mid-point between 4 and 5***
9	**Mid-point between 5 and 2***
10	Mid-point on the tip of R TP
11	Maximum posterior curve on the extreme of R TP
12	Most posterior point on the R posterior zygapophysis
13	Most posterior point on the L posterior zygapophysis
14	In posterior view, mid-point in the intersection between NA and NS
15	Mid-point on dorsal tip of NS
16	Maximum posterior curve on the extreme of L TP
17	Mid-point on the tip of L TP
18	Maximum anterior curve on the extreme of L TP
19	Most anterior point on the L anterior zygapophysis
20	Most anterior point on the R anterior zygapophysis
21	In anterior view, mid-point in the intersection between NA and NS
22	Maximum anterior curve on the extreme of R TP
23	Center of posterior epiphysis
24	Mid-point on dorsal border of posterior epiphysis*
25	Mid-point on R lateral border of posterior epiphysis*
26	Mid-point on ventral border of posterior epiphysis*
27	Mid-point on L lateral border of posterior epiphysis*
28	Mid-point between 24 and 25*
29	Mid-point between 25 and 26*
30	Mid-point between 26 and 27*
31	Mid-point between 27 and 24*
32	Intersection between radius and anterior border of NS (proximal)*
33	Intersection between radius and anterior border of NS (distal)*
34	Intersection between radius and posterior border of NS (proximal)*
35	Intersection between radius and posterior border of NS (distal)*

B)

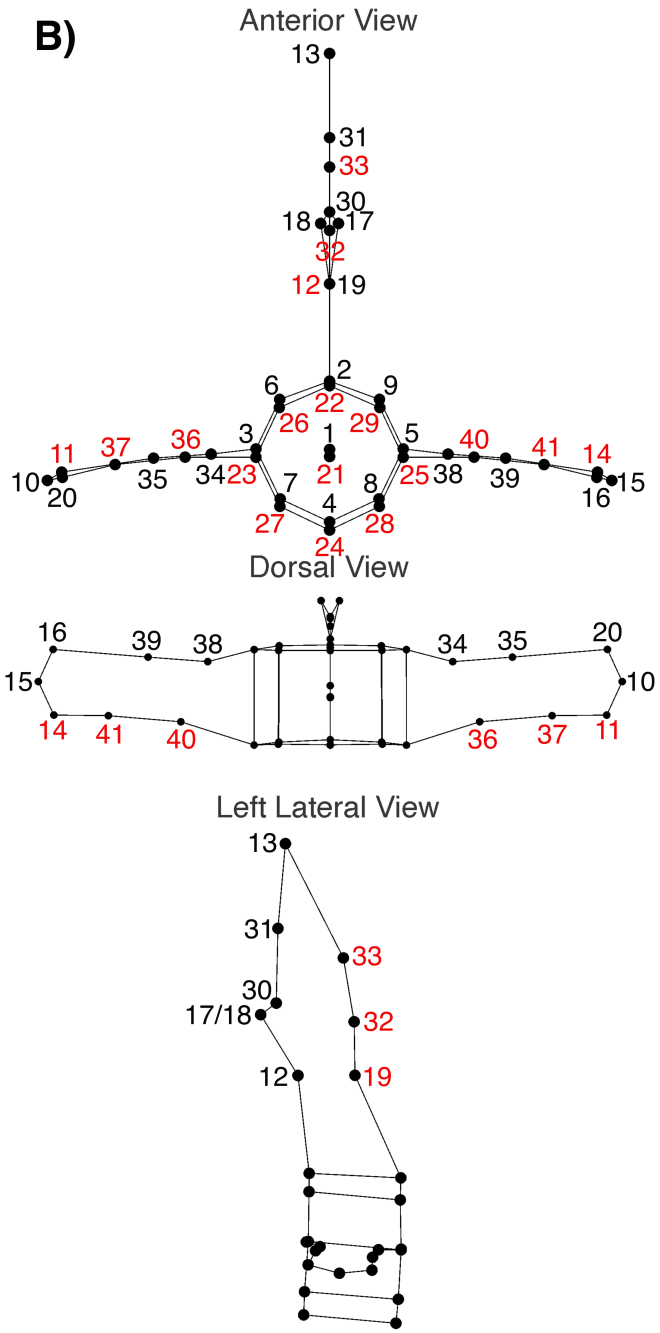

#	Description
1	**Center of anterior epiphysis**
2	**Mid-point on dorsal border of anterior epiphysis***
3	**Mid-point on R lateral border of anterior epiphysis***
4	**Mid-point on ventral border of anterior epiphysis***
5	**Mid-point on L lateral border of anterior epiphysis***
6	**Mid-point between 2 and 3***
7	**Mid-point between 3 and 4***
8	**Mid-point between 4 and 5***
9	**Mid-point between 5 and 2***
10	Mid-point on the tip of R TP
11	Maximum posterior curve on the extreme of R TP
12	In posterior view, mid-point in the intersection between NA and NS
13	Mid-point on dorsal tip of NS
14	Maximum posterior curve on the extreme of L TP
15	Mid-point on the tip of L TP
16	Maximum anterior curve on the extreme of L TP
17	Most anterior point on L metapophysis
18	Most anterior point on R metapophysis
19	In anterior view, mid-point in the intersection between NA and NS
20	Maximum anterior curve on the extreme of R TP
21	Center of posterior epiphysis
22	Mid-point on dorsal border of posterior epiphysis*
23	Mid-point on R lateral border of posterior epiphysis*
24	Mid-point on ventral border of posterior epiphysis*
25	Mid-point on L lateral border of posterior epiphysis*
26	Mid-point between 22 and 23*
27	Mid-point between 23 and 24*
28	Mid-point between 24 and 25*
29	Mid-point between 25 and 22*
30	Intersection between radius and anterior border of NS (proximal)*
31	Intersection between radius and anterior border of NS (distal)*
32	Intersection between radius and posterior border of NS (proximal)*
33	Intersection between radius and posterior border of NS (distal)*
34	Intersection between radius and anterior border of R TP (proximal)*
35	Intersection between radius and anterior border of R TP (distal)*
36	Intersection between radius and posterior border of R TP (proximal)*
37	Intersection between radius and posterior border of R TP (distal)*
38	Intersection between radius and anterior border of L TP (proximal)*
39	Intersection between radius and anterior border of L TP (distal)*
40	Intersection between radius and posterior border of L TP (proximal)*
41	Intersection between radius and posterior border of L TP (distal)*

C)

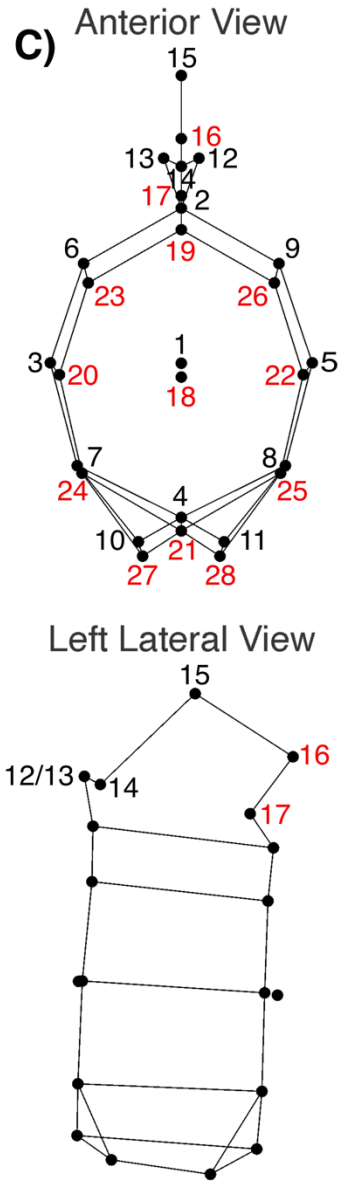

#	Description
1	**Center of anterior epiphysis**
2	**Mid-point on dorsal border of anterior epiphysis***
3	**Mid-point on R lateral border of anterior epiphysis***
4	**Mid-point on ventral border of anterior epiphysis***
5	**Mid-point on L lateral border of anterior epiphysis***
6	**Mid-point between 2 and 3***
7	**Mid-point between 3 and 4***
8	**Mid-point between 4 and 5***
9	**Mid-point between 5 and 2***
10	**In anterior view, ventral tip of R chevron anterior articulation facets**
11	**In anterior view, ventral tip of L chevron anterior articulation facets**
12	Most anterior point on L metapophysis
13	Most anterior point on R metapophysis
14	In anterior view, mid-point in the intersection between NA and NS
15	Mid-point on dorsal tip of NS
16	Maximum posterior curve on the extreme of NS
17	In posterior view, mid-point in the intersection between NA and NS
18	Center of posterior epiphysis
19	Mid-point on dorsal border of posterior epiphysis*
20	Mid-point on R lateral border of posterior epiphysis*
21	Mid-point on ventral border of posterior epiphysis*
22	Mid-point on L lateral border of posterior epiphysis*
23	Mid-point between 25 and 26*
24	Mid-point between 26 and 27*
25	Mid-point between 27 and 28*
26	Mid-point between 28 and 25*
27	In posterior view, ventral tip of R chevron posterior articulation facets
28	In posterior view, ventral tip of L chevron posterior articulation facets

Data S3. Examples of the scripts used for the analysis. A general example is given and particular modifications for regions are included.

```
library(geomorph)
library(RRPP)
library(Morpho)
library(ape)

# Loading data
Delphinidae_Data <- read.table("01Th_delphinidae_SoloAd.txt", header=T, dec =".")
Delphinidae_Clasif <-read.csv(file = "01Th_IDdelphinidae_SoloAd.csv", header = T,sep = ";",dec
= ".")
Delphinidae_Clasif$Sp<-as.factor(Delphinidae_Clasif$Sp)
Delphinidae_Clasif$Subfamily<-as.factor(Delphinidae_Clasif$Subfamily)
Delphinidae_Clasif$Habitat<-as.factor(Delphinidae_Clasif$Habitat)

# 3D array for Th
Delphinidae_3Darray <- arrayspecs(Delphinidae_Data[,2:ncol(Delphinidae_Data)], 35, 3)

# Semliankdmark matrix for Th
semilmk<-data.frame(before= c(2,6,3,7,4,8,5,24,28,25,29,26,30,27,21,32,15,35), slide=
c(6,3,7,4,8,5,9,28,25,29,26,30,27,31,32,33,35,34),
after=c(3,7,4,8,5,9,2,25,29,26,30,27,31,24,33,15,34,14))
semilmk<- as.matrix(semilmk)

# 3D array for ThTo, T and SP
Delphinidae_3Darray <- arrayspecs(Delphinidae_Data[,2:ncol(Delphinidae_Data)], 41, 3)

# Semliankdmark matrix for ThTo, Tm and SP
semilmk<-data.frame(before=
c(2,6,3,7,4,8,5,22,26,23,27,24,28,25,6,34,11,37,9,38,14,41,19,30,13,33), slide=
c(6,3,7,4,8,5,9,26,23,27,24,28,25,29,34,35,37,36,38,39,41,40,30,31,33,32),
after=c(3,7,4,8,5,9,2,23,27,24,28,25,29,22,35,20,36,26,39,16,40,29,31,13,32,12))
semilmk<- as.matrix(semilmk)

# 3D array for TS
Delphinidae_3Darray <- arrayspecs(Delphinidae_Data[,2:ncol(Delphinidae_Data)],28, 3)

# Semliankdmark matrix for TS
semilmk<-data.frame(before= c(2,6,3,7,4,8,5,19,23,20,24,21,25,22), slide=
c(6,3,7,4,8,5,9,23,20,24,21,25,22,26), after=c(3,7,4,8,5,9,2,20,24,21,25,22,26,19))
semilmk<- as.matrix(semilmk)

# GPA
Delphinidae_GPA <- gpagen(Delphinidae_3Darray,curves = semilmk,ProcD = FALSE )

# Data frame
gdf_delph<-
geomorph.data.frame(Delphinidae_GPA,SP=Delphinidae_Clasif$Sp,Subfamily=Delphinidae_C
lasif$Subfamily,Habitat=Delphinidae_Clasif$Habitat)

#Allometry
fit.Cs<-procD.lm(f1=gdf_delph$coords~log(gdf_delph$Csize), iter = 999,print.progress =
F,SS.type = "II",RRPP=TRUE)
summary(fit.Cs)

fit.common<-procD.lm(f1=gdf_delph$coords~log(gdf_delph$Csize) + gdf_delph$Subfamily,
iter = 999,print.progress = F,SS.type = "II",RRPP=TRUE)
summary(fit.common)

#Procrustes ANOVA
Delphinidae_Anova<-procD.lm(coords~SP, data =gdf_delph ,inter=10000,RRPP = TRUE)
summary(Delphinidae_Anova)
```

```
PW <- pairwise(Delphinidae_Anova, groups =gdf_delph$SP, covariate = NULL)
options(max.print=999999)
summary(PW, test.type = "dist", confidence = 0.95, stat.table = TRUE, option="max.print")

Delphinidae_AnovaRes<-procD.lm(fit.common$residuals~SP, data =gdf_delph
,inter=10000,RRPP = TRUE)
summary(Delphinidae_AnovaRes)

# Phylogeny used for Th, ThTo, Tm and SP
TreeDelphinidae<-
'((((((((((Slong,Sclym),Lhose),Ddelp),Scoeu),((Satte,Sfron),Ttrun)),Splum),Sfluv),((((Pelec,Fatte),
Gmacro),Ggris),Sbred)),((((Ccomm,Chect),((Laust, Lcruc),Cheav)),Lobsc),Liper)),Lalbi),Lacut);'
Delphinidae_phy<-read.tree(text=TreeDelphinidae)

# Species mean shapes for Th, ThTo, Tm and SP
Y1 <- mshape(gdf_delph$coords[,,which(gdf_delph$SP == "Slong")])
Y2 <- mshape(gdf_delph$coords[,,which(gdf_delph$SP == "Sclym")])
Y3 <- mshape(gdf_delph$coords[,,which(gdf_delph$SP == "Lhose")])
Y4 <- mshape(gdf_delph$coords[,,which(gdf_delph$SP == "Ddelp")])
Y5 <- mshape(gdf_delph$coords[,,which(gdf_delph$SP == "Scoeu")])
Y6 <- mshape(gdf_delph$coords[,,which(gdf_delph$SP == "Satte")])
Y7 <- mshape(gdf_delph$coords[,,which(gdf_delph$SP == "Sfron")])
Y8 <- mshape(gdf_delph$coords[,,which(gdf_delph$SP == "Ttrun")])
Y9 <- mshape(gdf_delph$coords[,,which(gdf_delph$SP == "Splum")])
Y10 <- mshape(gdf_delph$coords[,,which(gdf_delph$SP == "Sfluv")])
Y11 <- mshape(gdf_delph$coords[,,which(gdf_delph$SP == "Pelec")])
Y12 <- mshape(gdf_delph$coords[,,which(gdf_delph$SP == "Fatte")])
Y13 <- mshape(gdf_delph$coords[,,which(gdf_delph$SP == "Gmacro")])
Y14 <- mshape(gdf_delph$coords[,,which(gdf_delph$SP == "Ggris")])
Y15 <- mshape(gdf_delph$coords[,,which(gdf_delph$SP == "Sbred")])
Y16 <- mshape(gdf_delph$coords[,,which(gdf_delph$SP == "Ccomm")])
Y17 <- mshape(gdf_delph$coords[,,which(gdf_delph$SP == "Chect")])
Y18 <-mshape(gdf_delph$coords[,,which(gdf_delph$SP=="Laust")])
Y19 <- mshape(gdf_delph$coords[,,which(gdf_delph$SP == "Lcruc")])
Y20 <- mshape(gdf_delph$coords[,,which(gdf_delph$SP == "Cheav")])
Y21 <- mshape(gdf_delph$coords[,,which(gdf_delph$SP == "Lobsc")])
Y22 <- mshape(gdf_delph$coords[,,which(gdf_delph$SP == "Lipero")])
Y23 <- mshape(gdf_delph$coords[,,which(gdf_delph$SP == "Lalbi")])
Y24 <- mshape(gdf_delph$coords[,,which(gdf_delph$SP == "Lacut")])

# Species mean shapes for TS
Y1 <- mshape(gdf_delph$coords[,,which(gdf_delph$SP == "Slong")])
Y2 <- mshape(gdf_delph$coords[,,which(gdf_delph$SP == "Sclym")])
Y3 <- mshape(gdf_delph$coords[,,which(gdf_delph$SP == "Lhose")])
Y4 <- mshape(gdf_delph$coords[,,which(gdf_delph$SP == "Ddelp")])
Y5 <- mshape(gdf_delph$coords[,,which(gdf_delph$SP == "Scoeu")])
Y6 <- mshape(gdf_delph$coords[,,which(gdf_delph$SP == "Satte")])
Y7 <- mshape(gdf_delph$coords[,,which(gdf_delph$SP == "Sfron")])
Y8 <- mshape(gdf_delph$coords[,,which(gdf_delph$SP == "Ttrun")])
Y9 <- mshape(gdf_delph$coords[,,which(gdf_delph$SP == "Splum")])
Y10 <- mshape(gdf_delph$coords[,,which(gdf_delph$SP == "Sfluv")])
Y11 <- mshape(gdf_delph$coords[,,which(gdf_delph$SP == "Pelec")])
Y12 <- mshape(gdf_delph$coords[,,which(gdf_delph$SP == "Fatte")])
Y13 <- mshape(gdf_delph$coords[,,which(gdf_delph$SP == "Gmacro")])
Y14 <- mshape(gdf_delph$coords[,,which(gdf_delph$SP == "Ggris")])
Y15 <- mshape(gdf_delph$coords[,,which(gdf_delph$SP == "Sbred")])
Y16 <- mshape(gdf_delph$coords[,,which(gdf_delph$SP == "Ccomm")])
Y17 <- mshape(gdf_delph$coords[,,which(gdf_delph$SP == "Chect")])
Y18 <- mshape(gdf_delph$coords[,,which(gdf_delph$SP == "Lcruc")])
Y19 <- mshape(gdf_delph$coords[,,which(gdf_delph$SP == "Cheav")])
Y20 <- mshape(gdf_delph$coords[,,which(gdf_delph$SP == "Lobsc")])
Y21 <- mshape(gdf_delph$coords[,,which(gdf_delph$SP == "Lipero")])
Y22 <- mshape(gdf_delph$coords[,,which(gdf_delph$SP == "Lalbi")])
```

```
Y23 <- mshape(gdf_delph$coords[,,which(gdf_delph$SP == "Lacut")])
# Species mean shape array for Th
YT <- array(c( Y1, Y2, Y3, Y4, Y5, Y6, Y7, Y8, Y9, Y10, Y11, Y12, Y13,Y14, Y15,Y16, Y17, Y18, Y19,
Y20, Y21, Y22, Y23,Y24), dim = c(35,3,24), dimnames = list(c(),c(),Delphinidae_phy$tip.label))

# Species mean shape array for ThTo, Tm, SP
YT <- array(c( Y1, Y2, Y3, Y4, Y5, Y6, Y7, Y8, Y9, Y10, Y11, Y12, Y13,Y14, Y15,Y16, Y17, Y18, Y19,
Y20, Y21, Y22, Y23,Y24), dim = c(41,3,24), dimnames = list(c(),c(),Delphinidae_phy$tip.label))

# Species mean shape array for TS
YT <- array(c( Y1, Y2, Y3, Y4, Y5, Y6, Y7, Y8, Y9, Y10, Y11, Y12, Y13,Y14, Y15,Y16, Y17, Y18, Y19,
Y20, Y21, Y22, Y23), dim = c(28,3,23), dimnames = list(c(),c(),Delphinidae_phy$tip.label))

# Classifiers for species mean shapes
mean_Clasif <-read.csv(file = "ID_SoloAd.csv", header = T,sep = ";",dec = ".")
mean_Clasif$Sp<-as.factor(mean_Clasif$Sp)
mean_Clasif$Subfamily<-as.factor(mean_Clasif$Subfamily)
mean_Clasif$Habitat<-as.factor(mean_Clasif$Habitat)

# Classifiers for species mean shapes for TS
mean_Clasif <-read.csv(file = "TS_ID_SoloAd.csv", header = T,sep = ";",dec = ".")
mean_Clasif$Sp<-as.factor(mean_Clasif$Sp)
mean_Clasif$Subfamily<-as.factor(mean_Clasif$Subfamily)
mean_Clasif$Habitat<-as.factor(mean_Clasif$Habitat)

# Computing branch length for the phylogeny
Delphinidae_phy <- compute.brlen(Delphinidae_phy)

# Dataframe including species mean shapes and phylogeny
meanshape_gdf<-geomorph.data.frame(coords=YT, SP=mean_Clasif$Sp,
Subfamily=mean_Clasif$Subfamily,Habitat=mean_Clasif$Habitat,Phy= Delphinidae_phy)

# Phylomorphospace,
Delphinidae_PhyloMS<-gm.prcomp(A=meanshape_gdf$coords,phy =meanshape_gdf$Phy)

# Plots PC1 vs PC2
gp <- as.factor(paste(meanshape_gdf$Habitat))
levels(gp)
col.gp<-c( "purple","blue","red", "darkorange", "skyblue3","forestgreen" ,"darkgrey","gold")
names(col.gp) <- levels(gp)
col.gp<- col.gp[match(gp, names(col.gp))]
col.gp

plot(Delphinidae_PhyloMS, axis1=1, axis2= 2, phylo =TRUE,cex=1.1,pch=
c(22,22,22,22,22,22,22,22,22,22,21,21,21,21,21,24,24,24,24,24,24,24,23,23), col= "black", bg= col.gp,
phylo.par= list( tip.labels=FALSE, node.labels=FALSE, anc.states= FALSE, edge.color= "black",
edge.width= 0.9, tip.txt.cex =0.5, tip.txt.adj = c(-0.1, -0.1) ))

#Parameters for wirframe graphics
GPref<- gridPar(pt.bg = "white", pt.size =0.4, link.col="darkgray", link.lwd=1.3, tar.pt.bg =
"black", tar.pt.size = 1, tar.link.col = "black")

# Wireframe for Th
meanshape<-mshape(gdf_delph$coords)
frame <- matrix(c(1,1,10,10,
2,6,6,3,3,7,7,4,4,8,8,5,5,9,9,2,28,24,24,31,31,27,27,30,30,26,26,29,29,25,25,28,6,21,21,9,21,20,20,22,22,
10,10,11,11,12,12,14,14,13,13,16,16,17,17,18,18,19,19,21,14,31,14,28,14,34,34,35,35,15,
        15,33,33,32,32,21,6,28,3,25,7,29,4,26,8,30,5,27,9,31,2,24), ncol = 2, byrow = TRUE)

-       Wire frame for ThTo, Tm and SP:
frame <- matrix(c(1,1,21,21,2,6,6,3,3,7,7,4,4,8,8,5,5,9,9,2,22, 26,
26,23,23,27,27,24,24,28,28,25,25,29,29,22,6,34,34,35,35,20,20,10,10,11, 11,37,37,36,
36,26,29,40,40,41,41,14,14,15,15,16,16,39,39,38,38,9,
```

```
2,19,19,17,19,18,17,30,18,30,30,31,31,13,13,33,33,32,32,12,12,22,
2,22,6,26,3,23,7,27,4,24,8,28,5,25,2,22), ncol = 2, byrow = TRUE)

# Wire frame for ThTo, Tm and TS:
frame <-
matrix(c(1,1,18,18,2,6,6,3,3,7,7,4,4,8,8,5,5,9,9,2,19,23,23,20,20,24,24,21,21,25,25,22,22,26,26,19,2,14,
14,12,14,13,12,15,13,15,15,16,16,17,17,19,7,10,10,4,4,11,11,8,24,27,27,21,21,28,28,25,2,19,6,23,3,20,7,
24,10,27,4,21,11,28,25,8,22,5,26,9), ncol = 2, byrow = TRUE)

# Shape changes for minimum and maximum values of PC1 and PC2
#PC1
plotRefToTarget(M1=meanshape, M2=Delphinidae_PhyloMS$shapes$shapes.comp1$min,
gridPars= GPref, method="points", links=frame)
 plotRefToTarget(M1=meanshape,
M2=Delphinidae_PhyloMS$shapes$shapes.comp1$max,gridPars = GPref, method="points",
links=frame)

# PC2
plotRefToTarget(M1=meanshape, M2=Delphinidae_PhyloMS$shapes$shapes.comp2$min,
gridPars= GPref, method="points", links=frame)
plotRefToTarget(M1=meanshape,
M2=Delphinidae_PhyloMS$shapes$shapes.comp2$max,gridPars = GPref, method="points",
links=frame)
```

Data S4. Statistical significance of Z-scores for the pairwise comparisons, each semimatrix refers to a studied region: anterior thorax (Th), limit thorax-torso (ThTo), mid-torso (Tm), synclinal point (SP), and tailstock (TS). Species are arranged into subfamilies to improve visualization. Th: Thorax, ThTo: limit thorax-torso, Tm: mid-torso; SP: synclinal point; TS: tailstock. Significant Z-scores are in bold. Statistical significance is marked by asterisks; * $p < 0.05$; ** $p \leq 0.01$; *** $p \leq 0.001$. For abbreviations on species names see Figure 2.

	Th																							
ThTo	Lac	Lal	Dd	Lh	Sa	Sc	Sco	Sf	Sfr	Sl	Sp	Tt	Fa	Gg	Gm	Pe	Sb	Cc	Ch	Chc	La	Lc	Lp	Lo
Lac		**2.00***	**1.85***	0.65	**2.12***	**1.77***	1.55	**2.44****	**2.19***	1.27	**2.55****	**2.82****	**1.96***	**2.89*****	1.48	**3.12*****	**4.12*****	**3.99*****	1.18	0.55	**1.95***	**2.79****	**1.86***	**3.70*****
Lal	**1.87***		**2.12***	**1.90***	**1.95***	**2.15***	**2.00***	**2.14***	**2.11***	**2.18***	**1.70***	**2.94****	**1.91***	**2.27***	1.13	**2.19***	**2.99****	**2.57****	0.57	0.50	1.09	1.33	0.57	**1.72***
Dd	**1.84***	0.63		**2.17***	0.67	1.04	0.19	1.09	-0.19	**2.20***	1.09	1.40	1.29	**3.70*****	0.40	**3.50*****	**2.95****	**4.41*****	0.59	0.70	**2.06***	**2.61****	**2.04***	**3.10****
Lh	**2.27***	0.74	0.93		**2.10***	1.57	**1.75***	**2.62****	**2.32***	0.34	**2.81****	**2.87****	**1.85***	1.16	**2.00***	1.06	**3.74*****	**2.29***	1.02	-0.38	1.09	1.54	0.97	**2.84****
Sa	**3.53*****	**3.77*****	**4.13*****	**3.50*****		**1.99***	1.40	1.08	-0.52	**1.95***	0.33	1.31	-0.02	**2.34***	-0.25	**1.85***	**2.21***	**3.10****	**3.10****	0.25	**1.90***	**1.86***	**1.67***	**2.37***
Sp	**2.81****	**1.90***	0.78	0.83	**3.70*****		-1.48	**2.37****	1.21	0.41	1.67	**2.04***	**2.11***	**3.42*****	**1.77***	**2.68****	**3.21*****	**2.91****	0.06	-0.39	1.31	**1.93***	0.92	**1.98****
Sc	0.41	1.56	-0.20	1.42	**2.93*****	0.72		**2.17***	0.25	0.80	1.48	**1.87***	1.63	**2.98*****	1.38	**2.58****	**3.01****	**2.96****	0.05	-0.02	1.03	1.64	0.79	1.68
Sco	**2.39****	**2.69****	**2.08***	**2.47****	1.13	1.50	**1.69***		1.36	**2.84****	-0.17	0.16	0.85	**3.36*****	0.25	**2.82****	0.90	**3.24*****	0.75	1.30	**2.12***	**2.79****	**2.32***	**2.63****
Sf	1.44	**1.82***	0.97	**2.12***	**2.46****	**2.03***	0.51	1.23		**2.35****	0.32	0.84	0.74	**2.88****	0.24	**3.04****	**2.54****	**3.50*****	-0.38	0.61	**1.80***	**2.12***	1.53	**2.23***
Sfr	**2.71****	**3.25*****	**2.65****	**2.70****	1.51	**2.68****	1.36	0.92	0.35		**2.29***	**3.18****	**1.71***	**2.50****	**1.69***	**1.92***	**3.98*****	**3.31*****	0.19	-1.20	1.45	**1.81***	0.65	**3.21*****
Sl	**2.23***	**2.56****	**2.19***	**2.45****	1.38	1.45	**1.74***	0.23	**2.01***	**1.81***		-0.13	0.52	**2.59****	0.07	**1.78***	-0.57	**1.64***	-0.26	0.94	**1.56***	**1.67****	1.42	0.85
Tt	**2.84****	**2.11***	1.43	0.75	**3.48*****	1.55	1.57	1.53	**1.68***	**2.76****	**2.23***		**1.75***	**3.77*****	0.83	**3.23*****	**1.90***	**3.59*****	0.85	**1.59***	**2.67****	**3.32*****	**2.63****	**2.97****
Fa	**3.82*****	**3.79*****	**4.11*****	**3.14*****	**2.13***	**3.72*****	**2.75****	**2.28****	**2.83*****	**2.48****	**1.99***	**3.13*****		**2.13***	-0.98	**1.95***	**2.84****	**2.94****	-0.61	-0.02	1.50	**2.29***	**1.63***	**2.77*****
Gg	**1.97***	**2.41***	**3.47*****	**2.90*****	**3.35*****	**3.56*****	**2.70****	**2.84****	**2.87*****	**3.68*****	**1.81***	**3.79*****	**3.97*****		**1.39***	**2.03***	**4.53*****	**3.30*****	0.90	0.85	**2.28****	**1.83***	1.15	**3.38*****
Gm	**2.59****	**2.74****	**2.63****	**2.65****	**2.11***	**2.03***	**2.07***	1.37	**2.57****	**2.38****	-0.82	**2.21***	**1.87***	**2.17***		**1.78***	1.35	**2.27***	0.33	0.91	1.34	1.64	**1.81***	**1.71***
Pe	**3.17*****	**3.22*****	**3.34*****	**2.12***	**3.34*****	**2.59****	**1.83***	**2.19***	**3.04****	**2.67****	1.48	**2.34***	1.63	**3.71*****	1.01		**3.53*****	**1.73***	-0.64	1.70	1.55	1.59	0.57	**2.82****
Sb	**3.09*****	**3.24****	**3.53*****	**3.35*****	**2.46****	**3.42*****	**2.62****	**1.72***	**1.94***	**2.58****	**1.74***	**3.55*****	**3.85*****	**2.74****	**2.68****	**4.11*****		**4.07*****	1.03	1.85	**3.08****	**3.47*****	**2.65****	**2.76****
Cc	**2.21***	1.66	1.35	1.71	**3.47*****	**2.27****	1.17	**1.96***	0.90	**2.23***	**2.13***	1.65	**3.20*****	**3.43*****	**2.42****	**2.68****	**3.22*****		-2.36	-1.26	0.78	0.97	-0.98	1.65
Ch	0.35	0.07	-1.35	0.15	1.46	-1.23	-0.32	0.01	-0.57	0.35	0.95	-0.96	0.96	1.40	1.30	0.21	0.66	-1.14		-1.46	-1.60	-0.97	-0.87	-0.89
Chc	0.66	-0.03	-1.63	-0.04	**1.92***	-1.40	-0.26	0.28	-0.10	0.81	1.16	-0.54	1.60	**1.76***	1.62	0.76	0.91	-0.61	-3.23		-1.21	-0.88	-0.73	0.31
La	0.62	0.07	-0.49	1.25	**1.86***	0.25	-0.19	0.92	-0.78	0.82	1.23	0.67	**1.72***	1.53	**1.78***	1.35	0.60	-0.65	-1.52	-1.00		-0.36	-0.43	1.21
Lc	1.28	1.37	**1.99***	**2.30***	**4.63*****	**2.95*****	**1.68***	**2.98****	**2.24***	**3.56*****	**2.89****	**3.69*****	**4.56*****	**2.63****	**3.11*****	**4.82*****	**3.67*****	**3.18*****	1.13	0.98	**1.61***		-0.97	0.88
Lp	0.24	1.30	1.02	1.67	**3.34*****	**1.75***	0.68	**2.30****	1.68	**2.16***	**2.27***	**2.22***	**2.86*****	1.65	**2.42****	**2.29****	**2.58****	**1.92***	1.02	0.87	1.38	-0.43		-0.39
Lo	**2.04***	0.93	**2.62****	**2.29***	**5.18*****	**3.57*****	**2.73*****	**3.29*****	**2.83****	**4.16*****	**3.16*****	**3.87*****	**4.34*****	**2.62*****	**3.30*****	**5.34*****	**3.84*****	**3.62*****	1.09	1.16	**1.69***	0.21	0.95	

Data S4. Continuation

	Tm																						
SP	Lac	Lal	Dd	Lh	Sa	Sc	Sco	Sf	Sfr	Sl	Sp	Tt	Fa	Gg	Gm	Pe	Sb	Cc	Ch	Chc	La	Lc	Lp	Lo
Lac		0.29	**4.61*****	**2.03***	**2.96*****	**3.86*****	**3.82*****	**1.81***	**3.47*****	**4.33*****	1.64	**3.18*****	**2.80*****	1.63	**1.97***	**2.50****	**2.64*****	**3.58*****	**2.01***	0.56	0.52	**3.61*****	**2.10***	**3.68*****
Lal	**2.43****		**4.01*****	1.37	**2.41****	**3.50*****	**3.45*****	1.72	**2.98*****	**4.06*****	**1.82***	**2.87*****	**2.30***	1.36	**2.34****	**2.11***	**2.49****	**3.04*****	**1.73***	0.19	0.25	**2.98*****	**1.79***	**3.04*****
Dd	**2.62****	**2.20***		-0.38	1.52	-0.60	-1.24	**2.61****	**2.04***	0.47	**2.67*****	**2.12***	**2.76****	**3.37*****	**3.38*****	**3.61*****	**3.66*****	**3.71*****	0.29	1.54	1.02	-0.01	**2.49****	0.58
Lh	1.15	0.98	-0.36		-1.65	-0.95	-0.65	0.54	-1.30	-0.78	0.99	0.22	-0.25	0.71	**1.86***	0.90	1.26	0.44	-0.57	-0.32	-0.63	-1.44	0.71	-1.84
Sa	**4.04*****	**2.62****	**2.03***	-0.75		0.89	0.78	1.13	0.33	1.19	1.48	0.88	0.81	**1.81***	**2.38****	**1.97***	**2.28***	**2.02***	-0.62	-0.22	-1.02	0.06	**1.80***	0.05
Sp	**3.67*****	**2.44****	1.14	-0.82	-0.69		-0.80	**2.36****	1.09	-0.93	**2.43****	**1.92***	**2.05***	**2.98*****	**3.31*****	**3.00*****	**3.27*****	**3.39*****	0.53	1.39	0.80	-0.11	**2.16***	-0.03
Sc	**2.10***	**2.00***	0.67	-0.23	1.37	1.05		**2.11***	1.48	0.56	**2.29***	1.56	**1.98***	**2.72*****	**3.13*****	**2.70*****	**3.23*****	**3.03*****	-0.05	1.05	0.46	-0.86	**2.17***	0.03
Sco	**4.18*****	**3.50*****	**2.81*****	0.03	0.95	1.26	**2.16***		1.53	**2.27****	-1.17	0.70	0.65	0.65	0.36	0.84	-0.35	1.34	-0.09	-0.97	-0.48	**2.08***	**1.74***	**1.94***
Sf	**3.86*****	**3.11*****	**1.85***	-0.95	0.29	-0.70	**2.21***	1.29		0.96	**1.75***	**2.0***	1.51	**2.05***	**2.77*****	**3.01*****	**2.87*****	**3.25*****	0.60	0.77	-0.08	1.27	1.49	0.45
Sfr	**4.38*****	**3.17*****	1.54	0.32	**2.53****	0.86	**2.82*****	**2.53****	**1.75***		**2.53*****	**2.15***	**2.36****	**3.26*****	**3.20*****	**3.52*****	**3.52*****	**3.43*****	0.86	1.69	0.98	0.96	**2.17***	0.43
Sl	**2.79****	**3.95*****	**2.56****	**1.92***	**3.49*****	**2.97****	**2.34***	**2.21***	**3.40*****	**2.64****		0.68	0.85	0.90	-0.63	1.01	-0.58	1.41	0.25	0.01	0.07	**2.26***	**1.98***	**2.31****
Tt	**4.15*****	**3.52*****	**2.65****	0.66	**3.29*****	**2.51****	**3.13****	**1.98***	**2.85*****	1.56	1.34		1.43	**1.98***	**1.83***	**2.08***	**1.86***	**2.20***	-1.31	0.06	-0.44	**1.76***	**2.33****	**1.85***
Fa	**3.69*****	**3.61*****	**3.64*****	**2.74****	**4.02*****	**4.06*****	**3.21*****	**4.33*****	**4.90*****	**4.24*****	1.01	**3.46*****		1.02	**1.94***	**2.04***	**1.65***	**2.79*****	-0.11	-0.28	-1.20	**1.75***	**2.11***	**1.90***
Gg	**2.91****	**3.11*****	**3.12*****	**2.14***	**3.88*****	**3.40*****	**2.33***	**3.44*****	**4.17*****	**4.19******	1.49	**3.09****	-0.36		1.54	**2.03***	1.24	**2.57****	0.71	-0.18	-1.31	**2.57****	1.13	**2.43****
Gm	**3.27*****	**4.55*****	**3.28*****	**2.34***	**3.75*****	**3.47*****	**2.73****	**2.24***	**4.08*****	**3.76*****	-0.68	**2.50****	1.41	1.59		1.46	1.04	**1.88***	1.10	0.77	1.02	**3.00*****	**2.30****	**3.03*****
Pe	**2.51****	**2.34****	**2.68****	**2.19***	**4.32*****	**3.64*****	**3.05****	**4.40*****	**4.41*****	**3.61*****	**2.29***	**3.38*****	**2.05***	**2.21***	**3.20*****		**1.77***	1.59	-0.15	-1.50	-0.24	**2.48****	**2.29****	**2.76*****
Sb	**3.43*****	**3.94*****	**3.43*****	**1.79***	**3.56*****	**3.39*****	**2.15***	**2.14***	**4.03*****	**4.68*****	0.69	**3.53*****	**2.44****	**1.99***	0.46	**3.37*****		**2.81*****	0.15	-0.97	-0.88	**2.93****	**2.50****	**3.42*****
Cc	**2.68****	**3.43*****	**2.98****	0.49	**4.51*****	**3.96*****	**3.86*****	**3.80*****	**4.59*****	**4.55*****	**2.80****	**3.10*****	**5.40*****	**4.21*****	**3.52*****	**3.39*****	**4.03*****		-0.75	-0.73	0.03	**2.58****	**2.23****	**2.94*****
Ch	0.13	1.61	-1.12	-0.62	1.26	0.43	0.08	1.03	0.44	-0.34	0.27	-0.82	1.15	1.26	1.06	0.32	0.73	-1.50		-1.05	-1.04	-0.13	1.35	0.13
Chc	0.56	**1.72***	0.99	0.99	**2.85****	**2.38***	1.49	**2.48****	**2.72****	1.61	0.33	0.59	0.37	0.78	1.48	-0.94	1.36	0.29	-0.84		-1.46	0.68	1.14	0.79
La	0.08	0.96	-0.36	-0.12	**1.87***	1.03	0.59	**1.77***	1.35	0.19	0.67	-0.40	0.85	0.93	1.59	-0.73	1.26	-0.62	-1.57	-1.65		0.04	0.71	-0.05
Lc	-0.01	**2.55****	1.52	0.87	**3.31*****	**3.11*****	**2.05***	**3.55*****	**3.56*****	**3.21*****	**1.98***	**2.78****	**2.59****	**2.15***	**2.60****	**1.58***	**2.71****	0.55	-1.03	-0.33	-0.82		**2.02***	-0.72
Lp	0.35	1.32	1.32	0.01	**2.64****	**2.33****	1.59	**2.41****	**2.79****	**2.48****	**2.06***	**1.39***	**2.32****	1.39	**2.64****	1.21	**2.58****	-0.25	-0.33	-0.17	-0.59	-0.39		1.47
Lo	0.43	**2.45****	**1.68***	1.39	**3.95*****	**3.42*****	**1.99***	**3.74*****	**3.90*****	**3.63*****	**2.10***	**3.80*****	**2.84****	**2.61****	**2.45****	1.53	**2.63****	**2.02***	-0.17	0.17	-0.26	-0.50	1.02	

Data S4. Continuation.

TS	Lal	Dd	Lh	Sa	Sc	Sco	Sf	Sfr	Sl	Sp	Tt	Fa	Gg	Gm	Pe	Sb	Cc	Ch	Chc	Lc	Lp	Lo
Lac	0.82	**2.71*****	0.99	**2.51****	**3.16*****	**2.73*****	**2.80*****	**3.33*****	**3.55*****	**3.362*****	**3.73*****	**3.49*****	**3.54*****	**2.62*****	**2.26***	**3.47*****	**2.03***	0.99	-0.59	2.00	0.87	**2.77*****
Lal		**2.60*****	1.60	**2.53*****	**3.06*****	**2.67*****	**2.80*****	**3.13*****	**3.52*****	**3.39*****	**3.53*****	**2.94*****	**3.44*****	**2.85*****	**2.33****	**3.16*****	**2.58*****	1.45	0.61	**2.33****	1.55	**3.11*****
Dd			1.41	0.16	0.63	-1.03	1.17	0.53	1.62	1.84	**2.01***	1.63	**2.46****	1.10	1.54	1.81	**2.89*****	-0.18	1.41	1.64	-0.91	0.84
Lh				-0.91	-0.40	-0.92	-0.29	-0.39	-0.36	1.08	0.43	0.20	2.20*	0.11	0.04	0.32	0.84	-1.17	0.58	-026	-1.16	-1.12
Sa					-0.71	0.22	-0.32	-1.17	0.19	0.78	-0.26	0.77	1.36	0.51	**1.82***	0.43	**2.57****	-0.01	1.59	1.61	0.21	1.02
Sc						0.34	0.43	-0.14	-0.22	0.92	0.77	0.99	**1.73***	0.52	**2.36****	1.09	**3.14*****	0.68	**2.08****	**2.22***	0.40	1.45
Sco							0.98	0.46	1.33	1.79	1.68	0.89	**2.09***	0.78	1.46	1.37	**2.77****	0.42	1.54	**1.77***	-1.09	0.90
Sf								0.79	0.48	0.41	-0.50	0.37	0.65	-0.06	**1.86***	0.12	**2.48*****	0.36	1.56	1.46	0.13	0.91
Sfr									1.23	1.27	1.10	1.42	**2.15***	0.83	**2.42****	1.36	**3.62*****	0.62	**1.95***	**2.41****	0.12	1.97*
Sl										0.46	0.99	1.24	**1.77***	0.28	**2.76*****	1.37	**3.54*****	0.89	**2.40*****	**2.49*****	0.50	1.97*
Sp											0.12	1.10	0.64	0.03	**2.47****	0.79	**3.34*****	1.29	**2.47****	**2.34****	1.29	**1.90***
Tt												0.72	1.15	-0.11	**2.68****	0.55	**3.63*****	1.02	**2.30****	**2.46****	0.79	2.04*
Fa													1.11	-0.39	**2.04***	0.39	**3.22*****	0.84	**1.94***	**2.02***	-0.22	1.34
Gg														-0.59	**2.94*****	1.26	0.20	1.60	**2.49*****	**2.53****	0.96	2.20*
Gm															1.50	-0.14	**2.12****	0.44	1.69	1.29	-0.17	0.50
Pe																**2.64****	**2.07***	0.36	0.84	1.30	-0.63	1.25
Sb																	**3.39*****	0.78	**2.00***	**2.27****	0.07	**1.86***
Cc																		0.54	-0.79	0.92	0.41	**2.49****
Ch																			0.14	-0.22	-0.59	-0.30
Chc																				0.32	0.19	1.21
Lc																					-0.70	0.42
Lp																						-1.69

DataS5. Full description of the plots of PC1 versus PC2 for the five regions.

The distribution of the species along the first two principal components (PCs) revealed shape similarities between species with similar biomechanical requirements (Figure 3). At the same time, it evidenced certain degree of shape similarities between species of very dissimilar habitats. Changes along the first two PCs varied with the region but were mainly related with the length of the centrum, the size of its faces, and the development and orientation of processes and metapophyses (Figure 3). In all cases, the first two PCs explained over 58% of the total variance in vertebral morphology. The mid-torso and the tail stock showed the greatest percentages of explained variance, with 73.5% and 73.7%, respectively. The estimated common ancestor shape (ECA) is plotted, with most species showing varying divergence from this estimated shape depending on the region.

At the beginning of the thorax (Th), grouping for Lissodelphininae and Delphininae species seems to reflect the subfamily grouping, with most species within each subfamily being found in neighboring areas of the morphospace, although some showed particular morphologies (Figure 3). The ECA shape was located at origin of coordinates coinciding roughly with the consensus shape and being most similar to fast-swimming oceanic and shelf/oceanic species . In this region, Globicephalinae species were scattered in different areas of the morphospace, these differences were partially observed statistically (Data S4). The two most basal species, *Lagenorhynchus acutus* and *L. albirostris*, resulted to be separated in the morphospace, showing low values along PC1 but differing notably in PC2 values (Figure 3), with differences being statistically significant (Data S4). Maximum PC1 values represented long centra with slightly smaller faces, long robust neural processes, and short robust transverse processes with a less anterior inclination (Figure 4, Data S6). This area was occupied by three groups, differing in PC1 values: the coastal/riverine, *Sousa plumbea*, and the oceanic, *Steno bredanensis* ($PC1 >> 0$, $PC2 > 0$); the riverine *Sotalia fluviatilis* and the coastal *Tursiops truncatus* ($PC1 >> 0$, $PC2 < 0$); and the oceanic deep diver, *Globicephala macrorhynchus* (($PC1 >> 0$, $PC2 << 0$). These groups also varied in PC2 values, resulting in slight differences in centrum length and in the development and orientation of the processes (Figure 4). In this sense, maximum PC2 values signaled long centra with smaller faces, neural processes of average length but wider, and short robust transverse processes with a more anterior inclination (Figure 4, Data S6). On the other hand, minimum PC1 values were associated with short centra with large faces, short neural processes but long transverse processes (Figure 4, Data S6). It is worth mentioning that there were no statistical differences between species with positive PC1 values (Data S4). Minimum PC1 values were observed for *Lagenodelphis hosei* ($PC1 << 0$, $PC2 << 0$), and, together with *L. acutus*, clearly differed from the rest of the species showing similar negative PC2 values but differing in negative PC1 values (Figure 3). Most oceanic fast swimming and shelf Delphininae species were clustered relatively close to the origin of coordinates with negative PC2 values ($0 \cong PC1 < 0.05$, $PC2 < 0$). Vertebral shape for *Stenella coeruleoalba* and *S. clymene* resulted the most similar to the consensus, although with negative PC2 values (Figure 3). The remaining species of the subfamily Delphininae evidenced variation along both PC1 and PC2 with *Stenella frontalis* and *S. attenuata* showing the greatest PC1 values ($PC1 > 0$, $PC2 < 0$); and *S. longirostris* showing the most negative values on both PC ($PC1 < 0$, $PC2 < 0$). *Delphinus delphis* showed PC1 values similar to those of *S. frontalis* and *S. attenuate*, but with

slightly smaller PC2 values (Figure 3). Despite these qualitative differences, *D. delphis* was found not to be statistically different from *S. longirostris* and *L. hosei*. All Lissodelphininae, except *Lagenorhynchus obscurus*, were loosely grouped in the upper left quadrant (PC1 < 0, PC2 > 0). *L. obscurus* showed slightly positive PC1 values and *Cephalorhynchus heavisidii* slightly negative PC1 values, showing both similar values along PC2. On the contrary, *Cephalorhynchus hectori*, *Lagenorhynchus australis* and *L. cruciger* showed values associated with short centra, short neural processes and long transverse processes (PC1 < 0, PC2 > 0; Figure 3). *Lissodelphis peronii* (PC1 << 0, PC2 >> 0) differed notably from the rest of the subfamily, although those differences were not statistically significant (Data S4), with the most negative PC1 values and the greatest PC2 values of the subfamily. *Cephalorhynchus commersonii* shape fell in between *L. peronii* and *L. obscurus*. As mentioned above, Globicephalinae showed a great diversity of shapes. *S. bredanensis* was the species with the longest centra and neural process, followed by *G. macrorhynchus*. *Feresa attenuata* (PC1 > 0, PC2 < 0) showed shapes similar to *D. delphis and S. attenuata*. *Grampus griseus* (PC1 << 0, PC2 < 0) showed the lowest PC1 values for the subfamily. Finally, *Peponocephala electra* (PC1 < 0, PC2 > 0) showed values similar to those of *C. hectori* and *L. australis*.

In the limit between thorax and torso (ThTo), the coastal *L. australis* (PC1 ≅ 0, PC2 ≅ 0) was the closest to the origin of coordinates (Figure 3) and the ECA shape was located in proximity of this species as well as of some fast-swimming oceanic species. Maximum PC1 values evidenced compressed centra, small faces, slightly shorter neural spines, and long slender transverse processes (Figure 4, Data S6); and were represented by three different groups (Figure 3). One group comprised only of *L. hosei* (PC1 >> 0, PC2 >> 0), and resulting in overall small compressed centra with shorter neural spines (but overall well-developed neural processes based on centrum size), and long slender transverse processes with strong posterior inclination (Figure 3, Data S7). The second group, consisting in *L. albirostris* (PC1 >> 0, PC2 ≅ 0), with compressed centra and slightly larger faces, tall erect neural process, and long slender transverse processes. The third group consisted in by *L. peronii*, *L. obscurus*, and *L. cruciger*, with the first two species slightly differing in PC2 values with respect to the last one and evidencing variations in the length of the neural spine and in the inclination of transverse processes (Figure 3, Data S7). Despite these graphical differences, statistical differences were found only for the comparison between *L. hosei* and the two of three Lissodelphininae species (Data S4). In addition, the Lissodelphininae species showed differences most species with the exception of *L. acutus* and *L. albirostris*. I believe that lack of differences for some of *L. peronii* comparisons are influenced by the low number of specimens. Minimum PC1 values were found for *G. macrorhynchus* and *S. plumbea*, with different negative PC2 values but showing relatively long centra and short but robust transverse processes. All coastal species (Delphininae and Lissodelphininae) are grouped close to the center of the plot (PC1 ≅ 0) but showing different PC2 values. In this sense, *T. truncatus* showed the greatest PC2 values (Figure 3). This species was located close to the coastal Lissodelphininae *C. heavisidii*, but differed statistically only from Delphininae species in other quadrants of the morphospace (Data S4). Differences in PC1 and PC2 values suggest a longer centra and more robust processes in the *T. truncatus* than in *C. heavisidii*. Shelf and oceanic fast swimming Delphininae species, were scattered widely across the morphospace (Figure 3). *Delphinus delphis* showed the greatest PC1 values, resulting in the most compressed centra for the subfamily (Figure 3, Data S7). Three

Stenella spp. showed positive PC1 values, but differed in PC2 values, with *S. clymene* showing the greatest PC2 values, *S. coeruleoalba* showing PC2 values close to 0, and *S. frontalis* showing negative PC2 values. In this case, statistical differences were only found between species at the extremes of this PC2 values range with *S. clymene* being statistically different from *S. frontalis* but with *S. coeruleoalba* not differing from either (Data S4). Due to these differences *S. clymene* showed a relatively smaller centra, *S. coeruleoalba* had a shorter neural process than the other two species, and *S. frontalis* had the biggest centra and the longest neural process of the three (Data S7). Particularly, vertebral morphology for *S. clymene* resulted similar to the coastal *C. heavisidii*, although there were differences in the shape and length of the transverse processes (Data S7). The remaining *Stenella* species showed particular morphologies with respect to its congeners (Figure 3). In particular, *S. longirostris* was located closer to *some Globicephalinae* species than to any other *Stenella* spp, although there were statistical differences between them (Data S4). *S. attenuata* was the most particular one within the genus (PC1 < 0, PC2 < 0), evidencing relatively large elongated centra with long neural processes but short transverse processes. This species differed statistically from all other shelf and oceanic fast swimming Delphininae, with the exception of *S. longirostris* (Data S4). *L. albirostris* and *L. acutus* were statistically different (Data S4), and its PC values suggested differences in the degree compression (Data S6). In this sense, compressed smaller centra and well-developed slender processes were observed for *L. albirostris,* while *L. acutus* showed short centra, though longer than in *L. albirostris,* together with large faces and long robust processes (Data S7). Globicephalinae species had negative PC2 values except for the deep-diver *G. macrorhynchus* (PC1 << 0, PC2 > 0) and the oceanic fast swimming *P. electra* (PC1 < 0, PC2 > 0; Figure 3). This later species, showed long and overall large centra with relatively short neural processes but long robust transverse processes (Data S6). The three oceanic Globicephalinae species differed both in PC1 and PC2 values, with *F. attenuata* (PC1 < 0, PC2 < 0) being the most similar to *P. electra* but with negative PC2 values suggesting differences in the relative size of the centra, and in the development and orientation of the processes. At the other end, *G. griseus* values (PC1 > 0, PC2 << 0) resulted in the most compressed centra and longest processes for the subfamily, with transverse processes orientating almost perpendicularly to the antero-posterior axis (Figure 3; Data S7). Finally, *S. bredanensis* was located along a diagonal line between *F. attenuate* and *G. griseus*, with slightly negative PC1 values and intermediate PC2 values that suggest compressed centra, well developed neural processes and slightly shorter posteriorly inclined transverse processes (Figure 3; Data S7). Most Globicephalinae species differed statistically from all Delphininae species, except for species with negative PC1 values and positive PC2 values (*S. plumbea* and *S. fluviatilis*). Most species in this subfamily were statistically different form each other, except for *P. electra* when compared to *F. attenuata* and *G. macrorhynchus* (Data S4).

At the mid-torso (Tm), the oceanic *F. attenuata* showed the shapes closest to the consensus although it differed from it when analyzed closely (PC1 > 0, PC2 < 0; Figure 3). In this species, the axis of the centra changes, affecting inclination of the neural process (Data S7). In this region, the ECA morphology resulted most similar to an oceanic species. Maximum PC1 values were associated with longer and overall larger centra (Figure 4, Data S6) and represented by *G.*

macrorhynchus (PC1 >> 0, PC2 << 0), followed by *S. plumbea*, with both species showing distinct shapes in the morphospace (Data S6). Despite this, these species only showed statistical differences with species in different quadrants of the morphospace (Data S4). In the quadrant above, *L. acutus* and *L. albirostr*is shapes clearly differed from the rest of the species (PC1 >> 0, PC2 >> 0), although showing statistical differences only when compared to species in different quadrants of the morphospace (Data S4). *L. acutus* showed longer centra, larger faces and a more anteriorly inclined neural process (Figure 3; Data S7). Both species had long neural processes and relatively shorter transverse processes with posterior inclination. Most shelf and oceanic fast swimming species, disregarding the subfamily, were clustered along negative PC1 values signaling variable degrees of centrum compression, with some species showing positive PC2 values and some negative PC2 values (Figure 3) but not differing statistically from each other (Data S4). Minimum PC1 values were represented by *D. delphis* and three *Stenella* spp. (PC1 << 0, PC2 < 0). They all had highly compressed centra with small faces, and long slender transverse processes with anterior inclination. Despite this, there was variation in the relative size of the centra and the development and inclination of the neural process, with *S. longirostris* having the smallest faces and a neural spine with a strong anterior inclination (Data S7). On the other hand, *L. cruciger, L. obscurus, L. hosei*, and the other two *Stenella* species showed slightly less negative PC1 values and slightly positive PC2 values, except for *L. cruciger* and *S. attenuata* which showed PC2 values close to cero (Figure 3). The first three species (*L. cruciger, L. obscurus, and L. hosei*) showed variable compression of the centra with relatively large faces and long neural processes with strong anterior inclination (Data S7). Regarding *S. atenuatta* and *S. frontalis*, the centrum was longer than in the previous group, and *S. frontalis* had particularly small faces (smallest centra overall) but long neural processes (Data S7). Two oceanic fast swimming species, one belonging to Globicephalinae and one to Lissodelphininae, differ from this general trend (Figure 3). This way, *P. electra* was located close to the coastal *C. hectori* (PC1 > 0, PC2 ≅ 0) and to other Globicephalinae species, and *L. peronii* (PC1 < 0, PC2 << 0) diverged from all other species (Figure 3), although this was not so clearly evidenced statistically (Data S4). Despite their neighboring positions, *P. electra* had larger centrum faces and a shorter neural spine with stronger anterior inclination than *C. hectori* (Data S7). *L. peronii* resembled *L. albirostris* in its compressed centra with large faces and posteriorly inclined transverse processes, but differs form it showing relatively shorter neural processes and longer transverse processes. Coastal species formed a loose group around the origin of coordinates, varying both in PC1 and PC2 values (Figure 3). All Lissodelphininae coastal species showed some degree of centrum compression with variations in the development and inclination of the processes (Data S7), except for *C. heavisidii* that was highly similar to *T. truncatus* (PC1 < 0, PC2 > 0; Figure 3). Both species showed long centra and transverse process with strong anterior inclination, but *C. heavisidii* had larger centrum faces and shorter neural processes (Data S7). The oceanic *S. bredanensis* resulted similar to the riverine species *S. fluviatilis* (PC1 > 0, PC2 > 0; Figure 3). Both species had long centra, long robust neural processes and short transverse processes with an almost perpendicular orientation with respect to the antero-posterior axis. Despite this, *S. fluviatilis* had considerably longer centra and smaller faces (Data S7). *G. griseus* clearly differed graphically, although not always statistically, from other

Globicephalinae species (PC1 > 0, PC2 < 0), being located between two coastal species and the two shelf-oceanic species but clearly differing from both groups (Figure 3, Data S4). Shapes in this species reflected long centra, large centrum faces, changes in the orientation of the centrum axis with respect to the neural spine, and relatively short posteriorly inclined transverse processes (Data S7).

Shapes at the synclinal point (SP) showed groups that roughly coincided with the subfamilies, although there were species clearly differing from their closest relatives. At the same time, shape similarities between species from the same habitat categories but different subfamilies also evidenced certain degree of convergence between unrelated species, especially when considering coastal species (Figure 3). In this region, *C. heavisidii* was the closest to the consensus shape, and the ECA was close to this species and other coastal species. Maximum PC1 values were associated with long centra with small faces, short neural processes (associated with long neural arches but short neural spines), and long robust perpendicular transverse processes (Figure 4, Data S4). At maximum PC1 values, certain similarities were found between *G. macrorhynchus* and *S. plumbea*, differing in positive PC2 values (Figure 3). Despite these qualitative differences, they did not differ statistically from species in the same quadrant (Data S4). They both had long centra with the deep diver, *G. macrorhynchus*, showing longer and overall larger centra with notably shorter neural and transverse processes, and *S. plumbea* having long centra with relatively smaller highly convex faces and relatively larger processes (especially the transverse; Data S7). The riverine species *S. fluviatilis* (PC1 << 0, PC2 >> 0) qualitatively differed from other Delphininae species, showing long large centra with well-developed neural processes and robust but short transverse processes (Data S7). All Delphininae shelf and fast swimming species were grouped along negative PC1 values, with three *Stenella* spp. forming a group (PC1 << 0, PC2 > 0; Figure 3). Even though there were little statistical differences between these species, they differed mostly in the degree of centrum compression, with *S. attenuata* and *S. frontalis* having the longest centra, largest faces and longest neural spines but differing in the development of the transverse processes (Data S7). *L. hosei* qualitatively differed from the previous group in its PC2 values resulting in larger convex centrum faces (Figure 3). Differences in PC1 and PC2 values between S. *longirostris* and *S. coeruleoalba* resulted in the former species having shorter centra with notably smaller faces and an overall smaller centra (Data S7). *D. delphis* resembled *S. coeruleoalba* in PC1 values but it was the only Delphinninae species showing negative PC2 values (Figure 3), translating into large faces and a slightly compressed centra. In particular, *D. delphis* did not showed statistical differences when compared to other shelf or oceanic fast-swimming Delphininae species, except for *S. attenuate* and *S. frontalis*. *T. truncatus* differed greatly from its closest relatives (*S. frontalis*- *S. attenuate*; Data S4) and resulted similar to *C. heavisidii*, which differed in PC2 values with respect to other coastal Lissodelphininae species (Figure 3). Several Lissodelphininae species, disregarding their habitat, were grouped close to *L. acutus* (PC1 ≅ 0, PC2 < 0), showing variable degrees of centrum compression (Figure 3, Figure 4, Data S6). The coastal *C. hectori* (PC1 > 0, PC2 < 0) and the oceanic fast swimming *L. peronii* (PC1 ≅ 0, PC2 << 0) differed from this group only graphically (Figure 3, Data S4). *C. hectori* showed greater positive PC1 values associated with compressed centra with small faces (overall smaller centra) with short

neural processes and long transverse processes (Figure 3, Figure 4). *L. peronii,* had greater negative PC2 values signaling compressed centra with large faces, short neural processes (short neural spines) and long transverse processes. In this subfamily, coastal species tended to have longer centra or smaller centrum faces than shelf or oceanic fast swimming species (Data S7). *L. albirostris* (PC1 < 0, PC2 << 0), differed from other delphinids, showing certain similarities with *L. peronii*, but with highly compressed centra with large faces, long neural processes and shorter transverse processes (Data S7). Globicephalinae species did not show a clear grouping, although *G. griseus* and *F. attenuate* were grouped together (PC1 > 0, PC2 ≅ 0), with both species showing relatively long centra but with differences in the size of the faces which are smaller in the latter species (Figure 3, Data S7). *S. bredanensis* (PC1 > 0, PC2 > 0) showed particular morphologies with respect to all other Globicephalinae species, although statistical differences were not found for the comparison with *G. macrorhynchus* (Data S4), with longer vertebrae and larger centrum faces than the previous group (Figure 3, Data S7). Finally, *P. electra* also differed from other Globicephalinae (Data S4), being located close to Lissodelphininae species (PC1 > 0, PC2 < 0; Figure 3). This species had the most compressed centra and the longest transverse processes for the subfamily (Data S7).

As in the previous analyzed region, in the tailstock (TS) grouping appears to depict the subfamilies, but with certain clustering of species of similar habitats regardless of the subfamily and some species clearly diverging within each subfamily (Figure 3). In this region, shapes for *L. hosei* (PC1 > 0, PC2 ≅ 0) were the closest to the consensus shape although its centra showed some degree of both antero-posterior and lateral compression, as well as elongation in the dorso-ventral aspect (Data S7). The estimated common ancestral shape for this region showed relatively shorter centra than the consensus and similarity with a fast-swimming oceanic species and a coastal species. Maximum PC1 values were associated with a highly compressed centra with large flat faces and short neural processes (Figure 4). *L. albirostris* and *L. acutus* showed the maximum PC1 values, but differed in PC2 values, with the former species showing greater negative values. The differences in PC1 and PC2 values signal both greater lateral and antero-posterior compression, as well as a higher neural process in *L. albirostris* (Figure 3, Data S7). Despite this, these two species did not differ with each other nor with some Lissodelphininae species (Data S4). At the other end of the axis, minimum PC1 values were found for the coastal/riverine species *S. plumbea* (PC1 << 0, PC2 ≅ 0), being the most divergent shape within Delphininae with long centra and small highly convex faces (Figure 3, Data S7). Apart from this highly diverging species, Delphinidae species were loosely distributed along negative PC2 values, except for *S. fluviatilis* (PC1 < 0, PC2 > 0), and varied in PC1 values with three subgroups being distinguishable (Figure 3). Disregarding, this riverine species did not show statistical differences with respect to other Delphininae species. A subgroup including *L. hosei* (PC1 > 0, PC2 ≅ 0), *D delphis* (PC1 > 0, PC2 < 0) *and S. coeruleoalba* (PC1 ≅ 0, PC2 < 0; Figure 3). *L. hosei* had the largest and most convex faces of the three, *D. delphis* had the most compressed centra with large faces and *S. coeruleoalba* was the most similar to the consensus shape (Data S7). A second subgroup containing *T. truncatus* and the remaining *Stenella* species (*S. longirostris, S. clymene, S. attenuata* and *S. frontalis*). These four species differed both in PC1 and PC2 values, with low PC1

negative values associated with high PC2 negative values (Figure 3). This way, the coastal *Tursiops* showed the longest centra and the smallest faces of this subgroup (Data S7). All Lissodelphininae species were grouped together in the upper right quadrant (PC1 > 0, PC2 > 0) but without showing a clear clustering of habitats within the subfamily, although shelf and oceanic fast swimming species were located in neighboring areas of the morphospace (Figure 3). In this group, only *L. obscurus* statistically differed from the rest of the subfamily (Data S4). Two coastal *Cephalorhynchus* spp. (*C. commersonii* and *C. hectori*) showed the greatest PC1 values within the subfamily, resulting in the most compressed centra and the largest faces for the subfamily (Figure 3, Data S6, Data S7). Differences between these two species signaled a greater compression and convexity of the faces in *C. hectori*. The coastal *C. heavisidii* differed greatly from the other *Cephalorhynchus* species, showing lower values both on PC1 and PC2 and resulting in less compressed centra (both antero-posteriorly and laterally) and highly convex faces (Figure 3, Data S6). Finally, Globicephalinae species were widely distributed in the morphospace with *G. macrochynchus* and *G. griseus* located in neighboring areas (PC1 < 0, PC2 > 0) showing distinct shape with respect to the other species (Figure 3). Both these species had long but overall small centra with highly convex faces, especially *G. macrorhynchus* (Data S7). *F. attenuate* and *S. bredanensis* (PC1 < 0, PC2 ≅ 0), grouped together with the delphinid riverine species *S. fluviatilis*. They all had long centra but differed in the size of the faces, with the riverine species having the longest vertebrae, the largest faces and an almost circular cross section (centrum width similar to centrum height; Data S7). The oceanic fast swimming *P. electra* (PC1 > 0, PC2 ≅ 0), differed greatly from other Globicephalinae species, both graphically and statistically (Data S4), locating close to the oceanic fast swimming Lissodelphininae species but also to the coastal *C. heavisidii* (Figure 3). Once more, this species was the one that showed the most compressed centra (both antero-posteriorly and laterally) within the subfamily (Data S7).

Data S6. Shape changes for minimum and maximum PC values of the first two components (PC1 and PC2), with respect to consensus shape, for each vertebral region. Th: anterior thorax; ThTo: boundary thorax-torso; Tm: mid-torso; SP: synclinal point: TS: tailstock. Ant.: anterior; A-P: antero-posterior axis; D-V: dorso-ventral axis; d-v: dorso-ventral; Incl.: inclination; NA: neural arch; NP: neural process; NS: neural spine; Post.: posterior; TP: transverse processes; ⊥: perpendicular to; +: more; **-** : less. See Figure 4.

	PC1		PC2	
	Negative	**Positive**	**Negative**	**Positive**
Th				
Centrum	Shorter	Longer (A-P)	Shorter	Longer
Faces	Larger. Convex Ant. face	Slightly smaller. Concave Ant. face	Larger	Smaller
NP	Notably shorter, + Post. Incl.	Longer, robust. + Ant. Incl	Average length, narrower. Longer NA. Shorter NS. + Post. Incl.	Average length, wider. **-** Post. Incl.
TP	. Longer, slender. Extremes + dorsal. **-** Ant. Incl.	Shorter, wider. Extremes + ventral. + Ant. Incl	Slightly longer, narrower. Extremes + ventral. **-** Ant. Incl.	Slightly shorter, wider. Extremes + dorsal. + Ant. Incl.
ZP	**-** developed	+ developed	Closer to A-P Pre-ZP and Post-ZP **-** developed	Further from A-P Pre-ZP and Post-ZP well developed
ThTo				
Centrum	Longer	Shorter	Slightly shorter	Longer
Faces	Larger	Smaller	Average	Smaller centra over all
NP	Longer, robust (notably larger NA)	Shorter, slender.	Longer. **-** Post. Incl.	Shorter (short NS). + Post. Incl.
TP	Shorter, wider - Post. Incl.	Longer, slender. **+** Post. Incl.	Average lenght. **-** Post. Incl.	Longer, slender + Post. Incl.
MP	**+** developed Higher. Further from A-P	**-** developed Lower. Closer to A-P	- developed Lower. Closer to A-P	+ developed. Higher. Further from A-P
Tm				
Centrum	Shorter	Notably longer	Notably longer.	Highly compressed A-P.
Faces	Smaller centra over all	Larger centra over all	Smaller.	Larger.
NP	Longer. slender. Long NS + Ant. Incl.	Shorter, robust. Short NS. - Ant. Incl.	Average length, robust. Almost ⊥ to A-P	Slightly shorter, slender. - Ant. Incl.
TP	Longer, slender + Ant. Incl.	Shorter, wider Post. Incl.	Average length, robust. Slight Post. Incl.	Average length, slender. Strong Post. Incl.
MP	Small/absent.	+ developed. Higher	+ developed. Higher	- developed, Lower
SP				
Centrum	Slightly Shorter	Longer	Highly compressed A-P.	Notably longer.
Faces	Larger	Smaller	Larger	Smaller

NP	Longer, robust. Short NA ⊥ to A-P.	Shorter, narrower. Long NA + Ant. Incl.	Longer, narrower. + Ant. Incl.	Longer, robust. ⊥ to A-P.
TP	Slender, + Ant. Incl.	Longer, robust. ⊥ to A-P.	Longer, narrower	Shorter, wider.
MP	- developed. Lower.	+ developed. Higher.	+ developed. Higher. Further from A-P	Well developed, Lower. Closer to A-P
TS				
Centrum	Notably long A-P. Laterally compressed	Highly compress A-P.	Slightly shorter. Lateral compression	Longer. Width ≅ Height.
Faces	Smaller. Highly convex	Notably Larger. Flat	Smaller. Flat	Larger. Convex
NP	Especially well developed	Shorter.	Larger. Robust. ⊥ to A-P.	Shorter. + Post. Incl.
MP	Present	Present. Lower	Present. Lower	Well developed.
CF	Ant.: Slightly smaller Post.: Slightly smaller	Ant.: average Post.: smaller	Ant.: Slightly smaller Post.: Slightly smaller	Ant.: slightly larger Post.: slightly larger

Data S7. Species specific shapes (black) compared to the consensus shape (grey) for the five regions along the vertebral column of 24 species of dolphins. Anterior (A), dorsal (D) and left lateral (L) views are included. A and B) Th: anterior thorax; C and D) ThTo: limit between the thorax and the torso; E and F) Tm: mid-torso; G and H) SP: synclinal point; I) TS: tailstock.

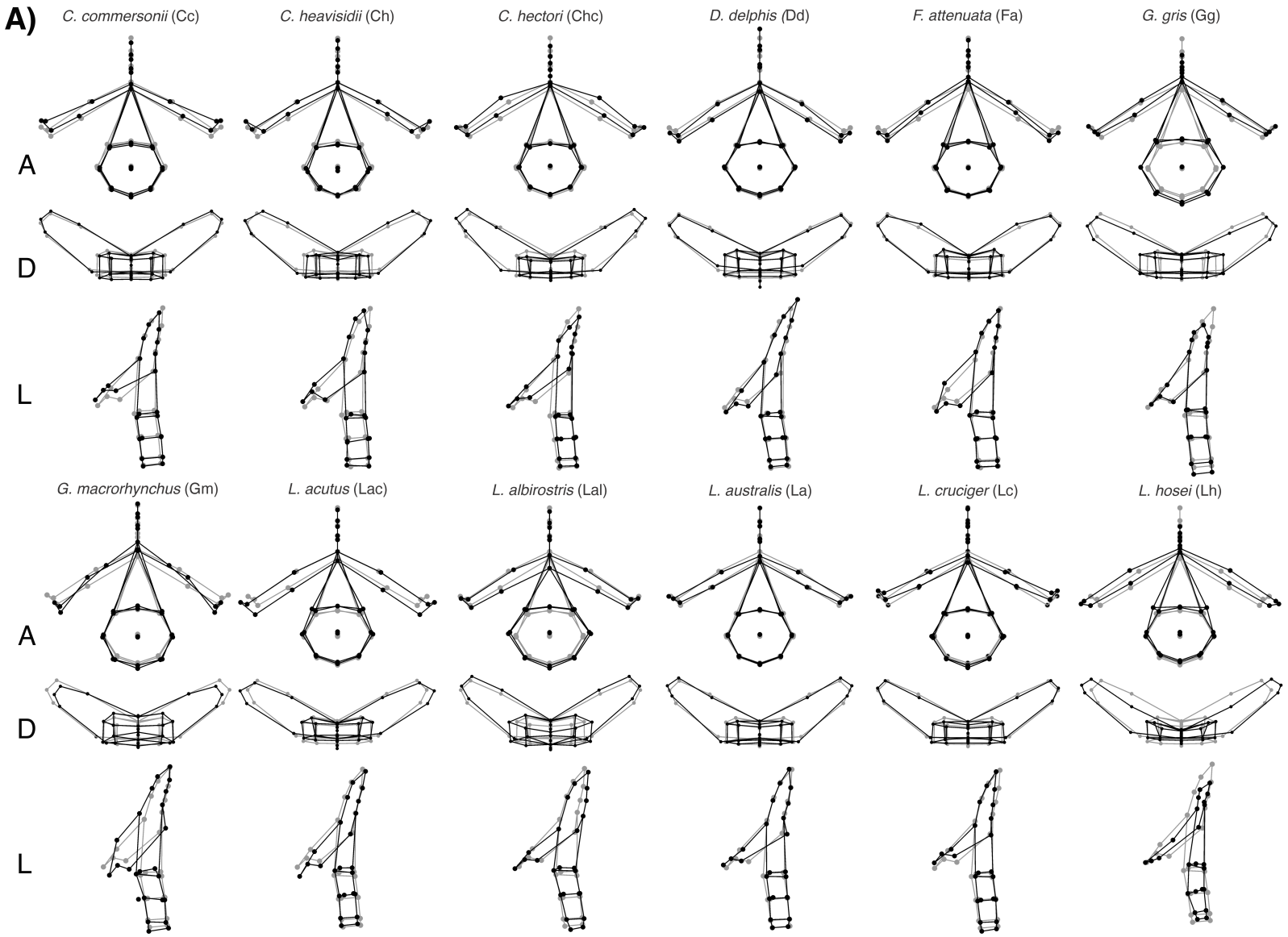

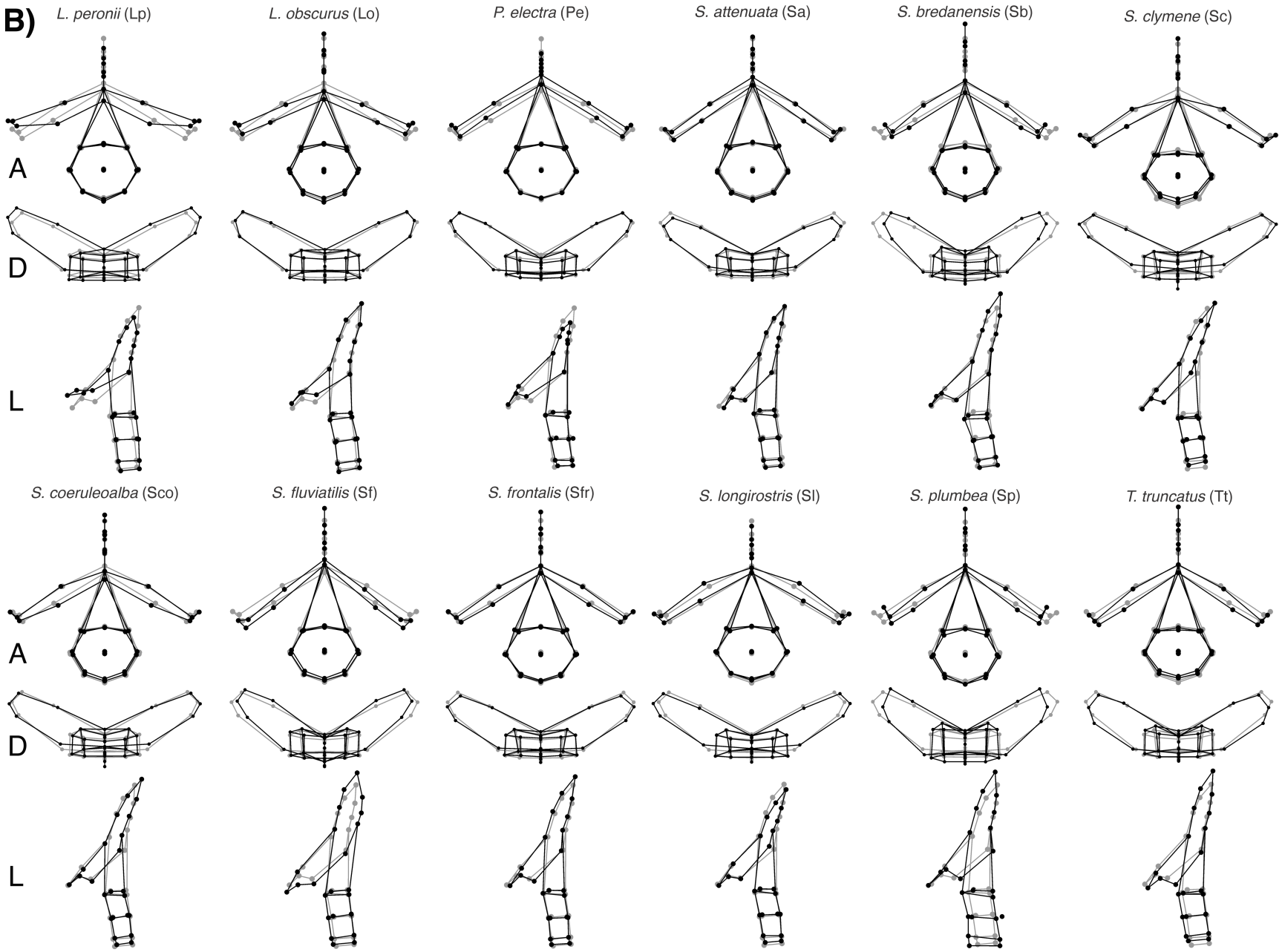

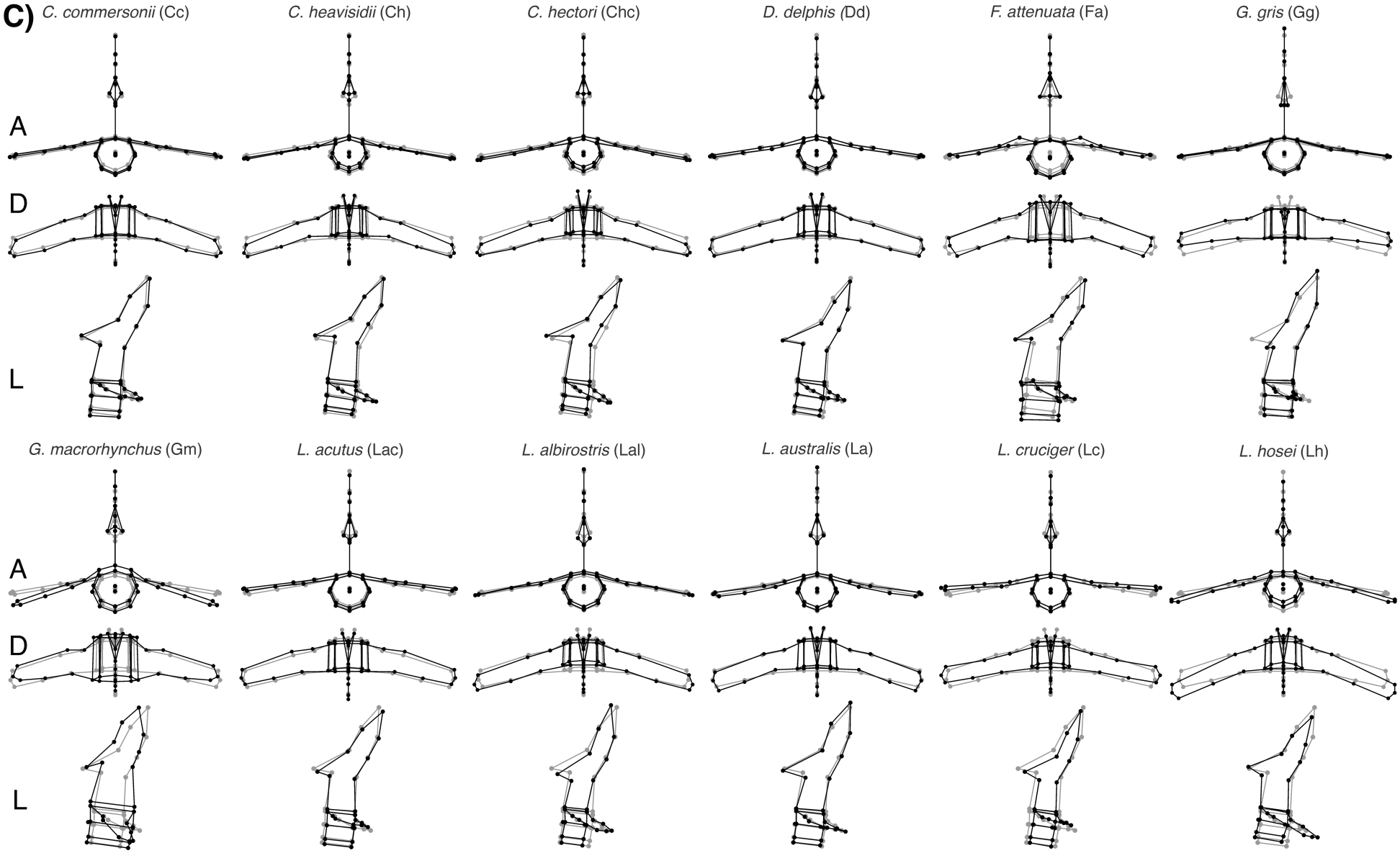

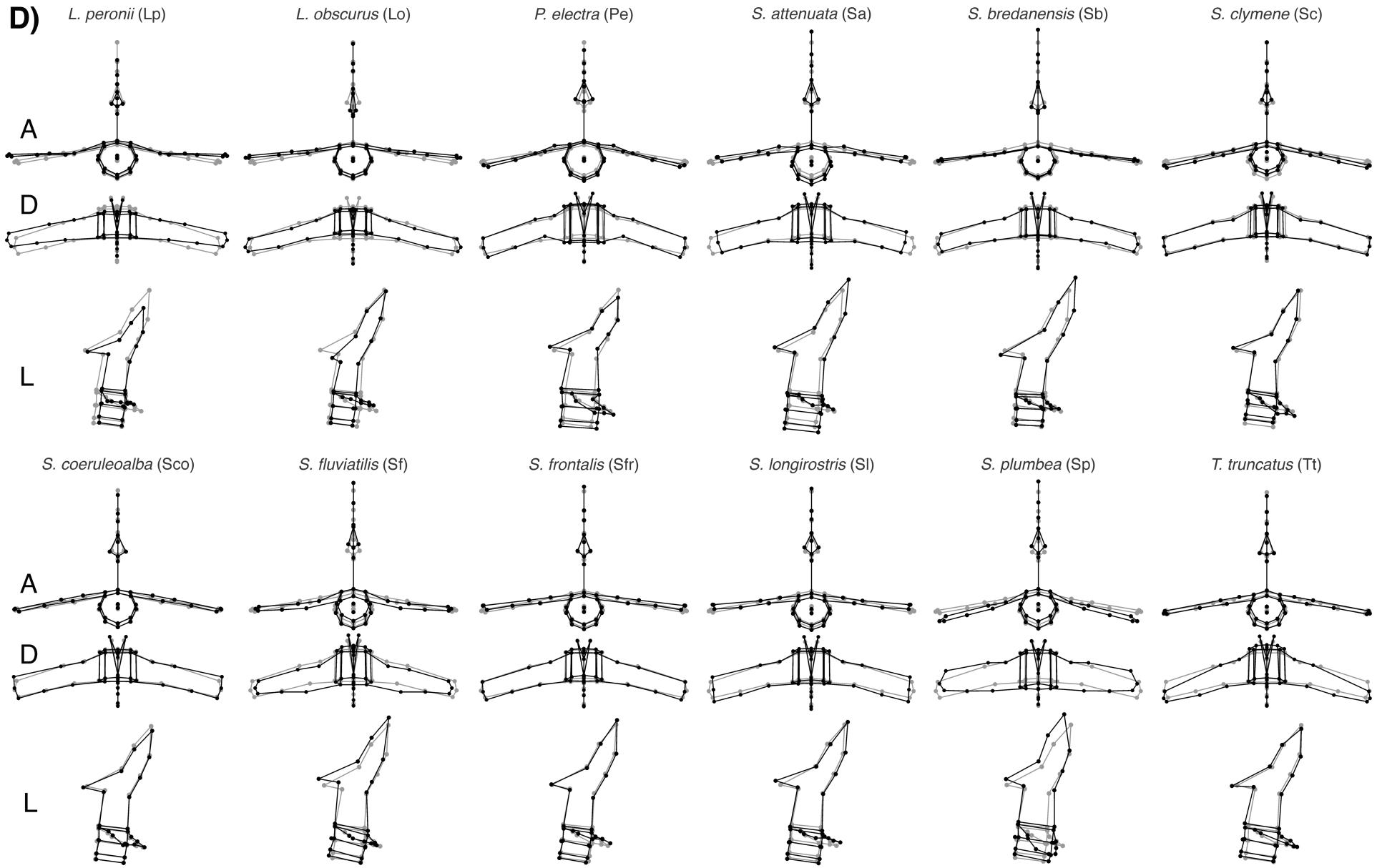

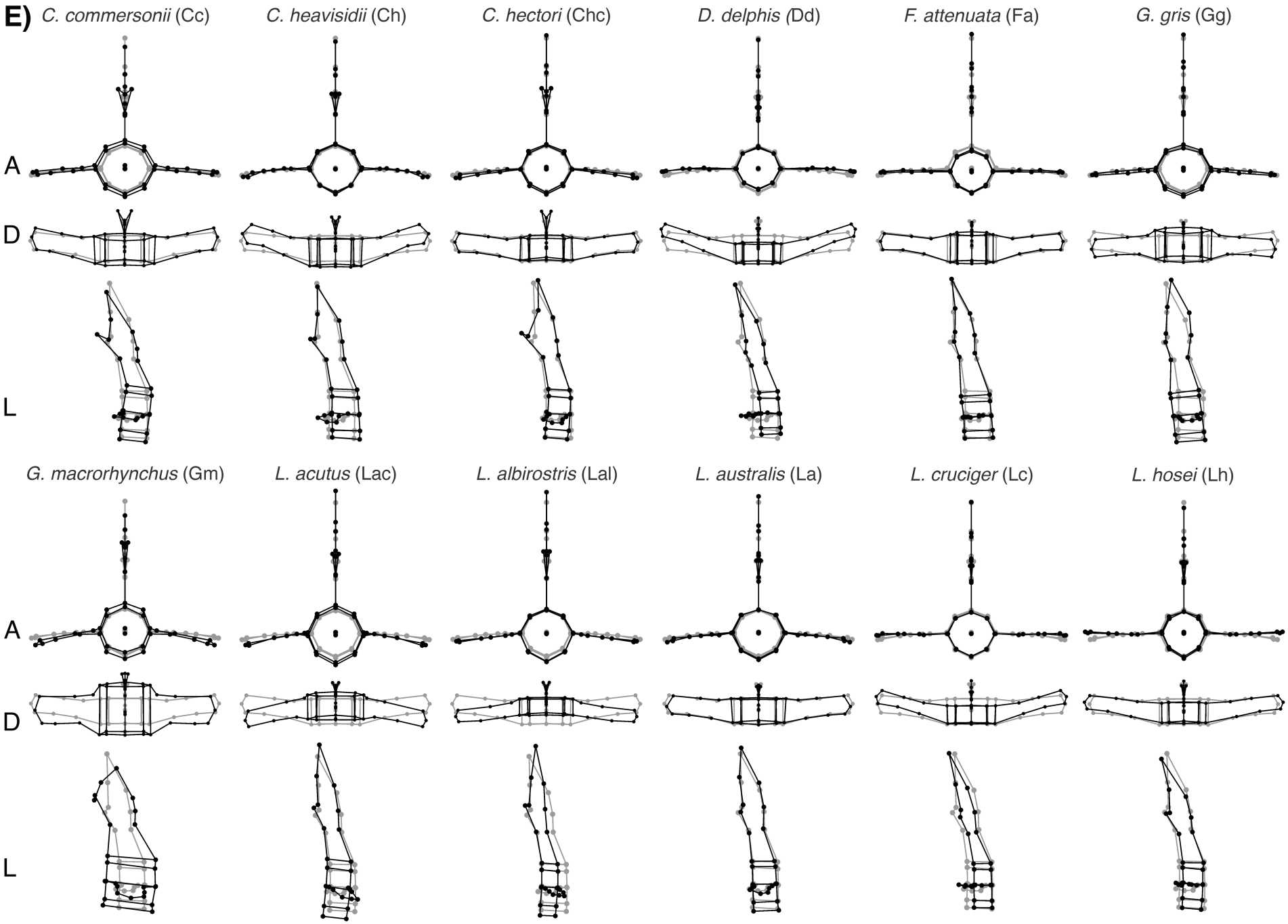

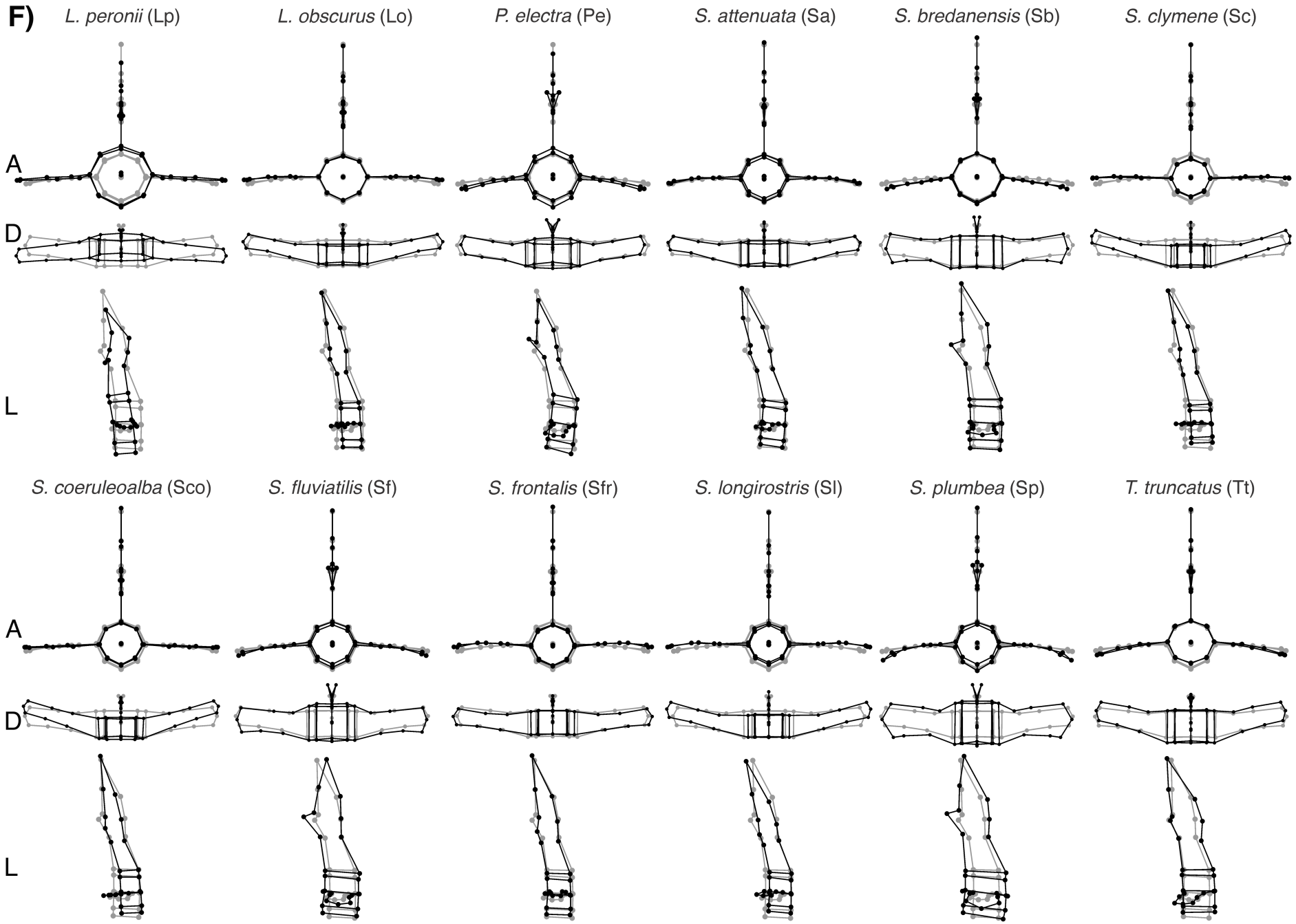

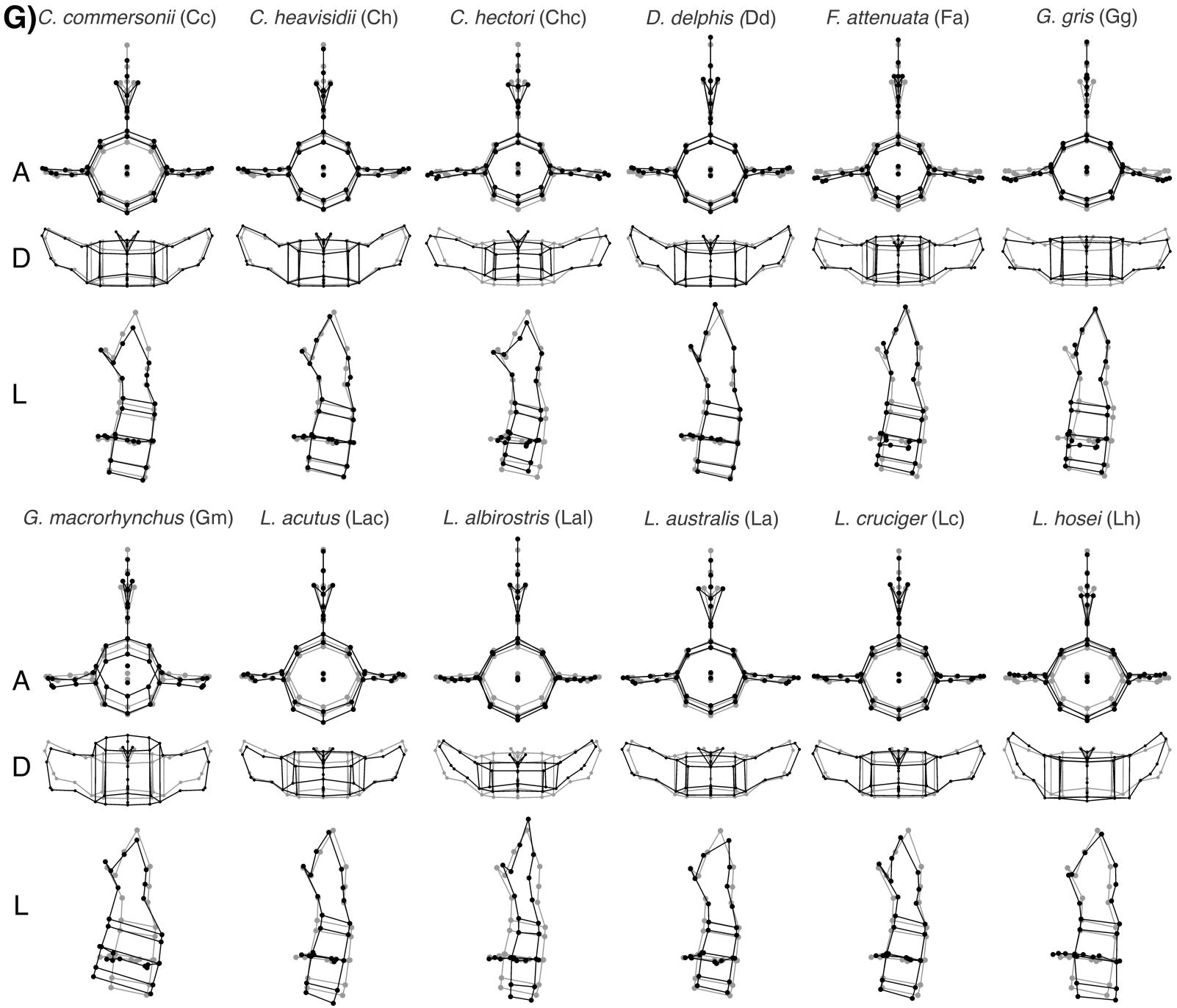

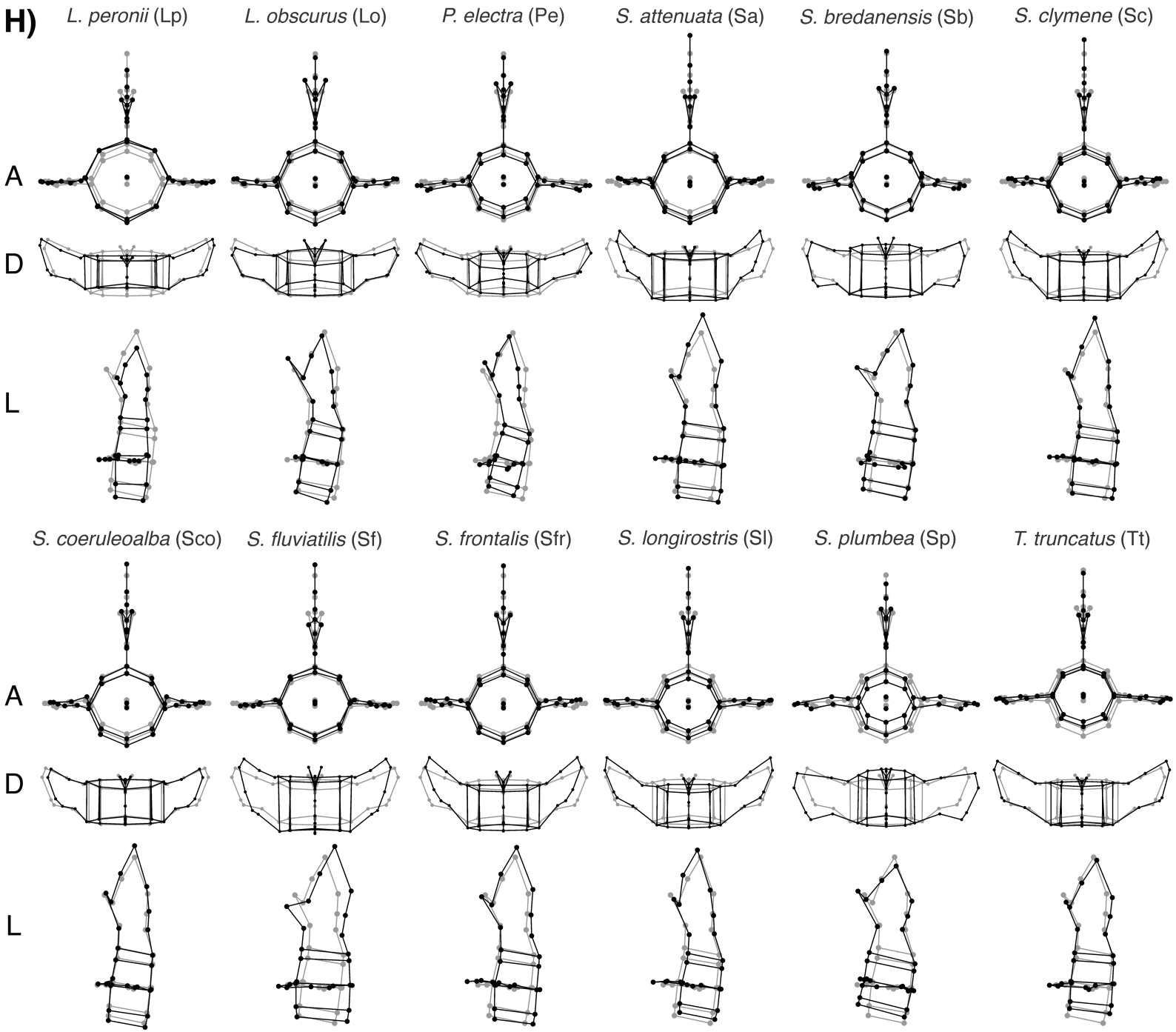

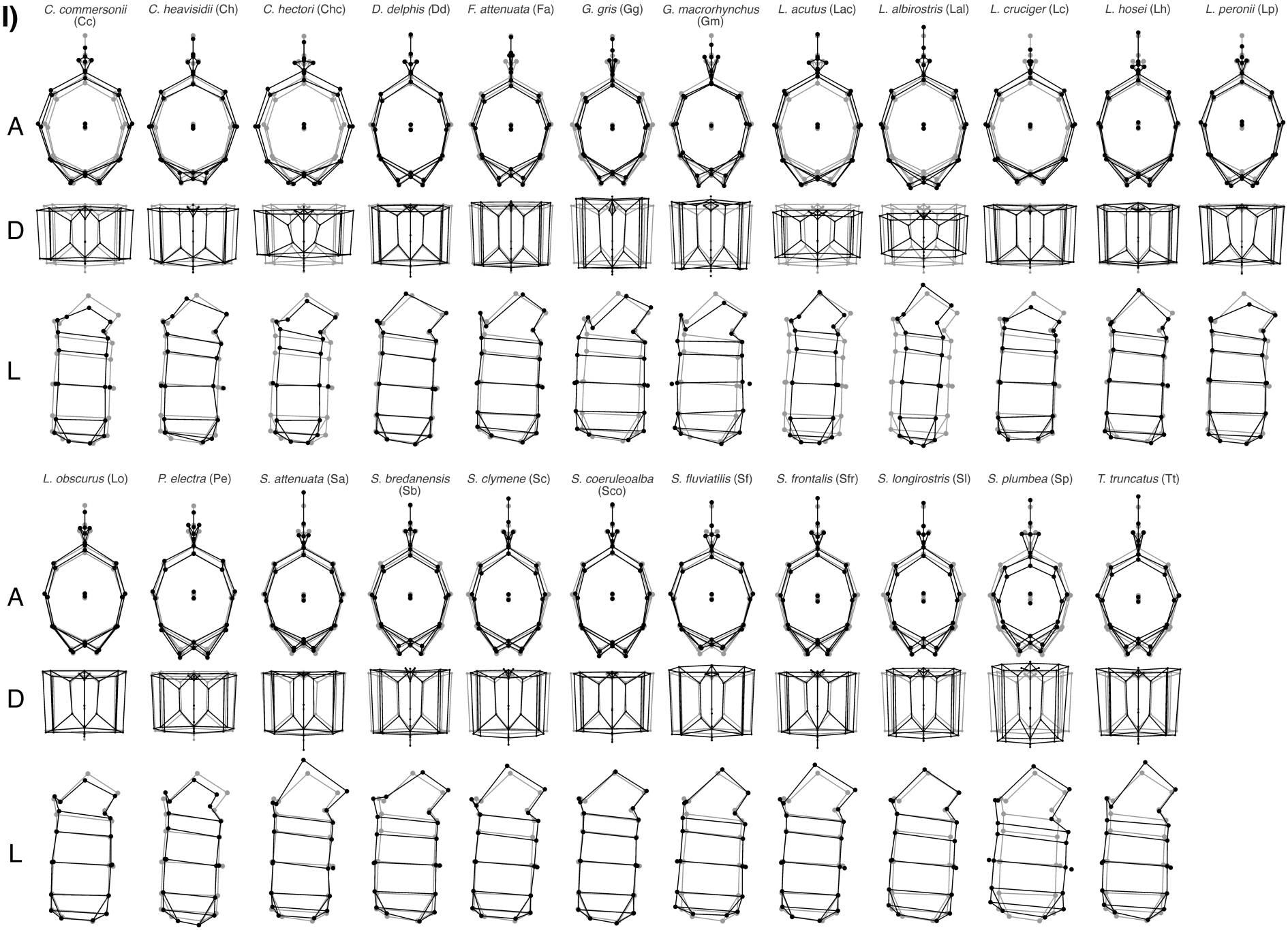

This preprint was submitted under the following conditions:

- The authors declare that they are aware that they are solely responsible for the content of the preprint and that the deposit in SciELO Preprints does not mean any commitment on the part of SciELO, except its preservation and dissemination.
- The authors declare that the necessary Terms of Free and Informed Consent of participants or patients in the research were obtained and are described in the manuscript, when applicable.
- The authors declare that the preparation of the manuscript followed the ethical norms of scientific communication.
- The authors declare that the data, applications, and other content underlying the manuscript are referenced.
- The deposited manuscript is in PDF format.
- The authors declare that the research that originated the manuscript followed good ethical practices and that the necessary approvals from research ethics committees, when applicable, are described in the manuscript.
- The authors declare that once a manuscript is posted on the SciELO Preprints server, it can only be taken down on request to the SciELO Preprints server Editorial Secretariat, who will post a retraction notice in its place.
- The authors agree that the approved manuscript will be made available under a Creative Commons CC-BY license.
- The submitting author declares that the contributions of all authors and conflict of interest statement are included explicitly and in specific sections of the manuscript.
- The authors declare that the manuscript was not deposited and/or previously made available on another preprint server or published by a journal.
- If the manuscript is being reviewed or being prepared for publishing but not yet published by a journal, the authors declare that they have received authorization from the journal to make this deposit.
- The submitting author declares that all authors of the manuscript agree with the submission to SciELO Preprints.